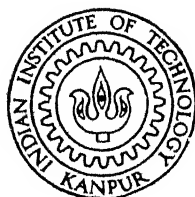


ELECTRICAL PROPERTIES OF SOME OXIDE-BASED SEMICONDUCTING SWITCHING GLASSES

By

ASIS KUMAR BANDYOPADHYAY



ME
1974

TH
ME/1974/M
B223e

M
BAN/669.9
B223e
ELE

DEPARTMENT OF METALLURGICAL ENGINEERING

INDIAN INSTITUTE OF TECHNOLOGY KANPUR

APRIL, 1974

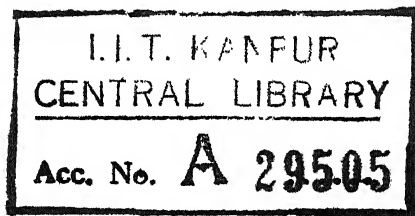
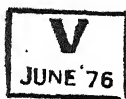
ELECTRICAL PROPERTIES OF SOME OXIDE-BASED SEMICONDUCTING SWITCHING GLASSES

**A Thesis Submitted
In Partial Fulfilment of the Requirements
for the Degree of
MASTER OF TECHNOLOGY**

6/5/74

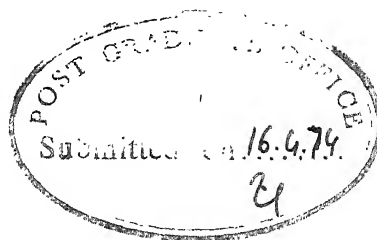
**By
ASIS KUMAR BANDYOPADHYAY**

**to the
DEPARTMENT OF METALLURGICAL ENGINEERING
INDIAN INSTITUTE OF TECHNOLOGY KANPUR
APRIL, 1974**



3 JUN 1974

ME-187A-M-BAN-ELE

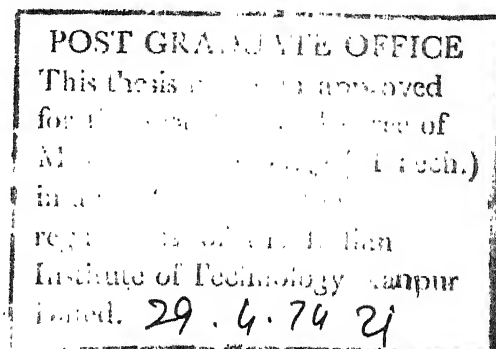


ii

CERTIFICATE

Certified that this work on 'Electrical Properties of Some Oxide-Based Semiconducting Switching Glasses' by A.K. Bandyopadhyay has been carried out under my supervision and that this has not been submitted elsewhere for a degree.

D. Chakravorty
(D. Chakravorty)
Associate Professor
Department of Metallurgical Engg.,
Indian Institute of Technology, Kanpur



ACKNOWLEDGEMENTS

I wish to express my sincere thanks and gratitude to Dr. D. Chakravorty for his inestimable help and valuable guidance which were responsible for the successful completion of the thesis.

I am thankful to Mr. A.N. Tiwari for some stimulating discussions during the course of preparation of this thesis. My sincere thanks are due to my colleagues for their help during the progress of the work.

I sincerely acknowledge the help rendered by Mr. B. Sharma and Mr. R.K. Prasad of Ceramics Lab. and Mr. L.S. Gupta of Integrated Circuits Lab.

I am indebted to M/S Pilkington Brothers Ltd., (U.K.) for supporting this investigation.

Last but not the least, my hearty thanks are due to Mr. J.K. Misra for his excellent typing and Mr. A.K. Ganguly for drawing the figures.

Asis Kumar Bandyopadhyay

SYNOPSIS

✓ The main theme of the present investigation springs out of the fact that $\text{Na}_2\text{O} - \text{B}_2\text{O}_3 - \text{SiO}_2 - \text{Bi}_2\text{O}_3$ glass has shown memory switching characteristics and hence the basic mechanism of semiconduction in this glass needs to be studied. This glass and another bismuth containing glass were studied in the present work. ✓

(The electrical conductivity measurement with temperature suggests that there are two mechanisms operative, namely electronic and ionic, in two distinct temperature regions for both the glasses. The ionic conductivity in the high temperature region is ascribed to the field induced drift of Na^+ ions through the glass structure and the electronic conductivity in the low temperature region is associated with the presence of bismuth in the glass structure, which has been substantiated by the observation of only ionic conductivity in two non-bismuth glasses of the above two systems.)

The basic mechanism for electronic conduction is ascribed to phonon-assisted hopping of charge carriers (i.e. electrons) from one localised state to another from the frequency dependence of conductivity at lower temperature, whether the hopping is between nearest neighbours or between distant sites cannot be answered at this state. However, it can be roughly said that the picture of electron tunnelling between

nearest sites is more prominent than distant ones because of more conformance of the present data with the T^{-1} behaviour than $T^{-1/4}$ behaviour. It is thought that in the temperature of investigation nearest neighbour optical phonon hopping is operative where $\sigma(\text{ac}) \ll \sigma(\text{opt})$.

From the frequency dependence of conductivity in the lower temperature region it seems likely that the conductivity is due to the transport ^{of} small polarons. The analysis of the dielectric properties show that there is a distribution of relaxation time. There is a correspondence of the activation energy due to relaxation process with the activation energy of electronic conduction.

CONTENTS

<u>CHAPTER</u>	<u>Page</u>
CERTIFICATE	ii
ACKNOWLEDGEMENTS	iii
SYNOPSIS	vi
I. INTRODUCTION	1
1.A Switching in Amorphous Solids	2
1.A.1 Introduction	2
1.A.2 General Device Characteristics	3
1.A.3 Threshold and Memory Switching	4
1.A.4 Mechanisms of Switching	7
1.A.5 Switching in Oxide Glasses	9
1.A.6 Conclusion	10
1.B Semiconductivity in Amorphous Materials	11
1.B.1 Introduction	11
1.B.2 Anderson's Localization Theory	12
1.B.3 Mott's Hypothesis of Conduction	16
1.B.4 A Comparison Between Crystalline and Amorphous Semiconductors	19
1.B.5 Some Characteristics of Amorphous Semiconductors	21
1.B.6 Classification and Description about Amorphous Semiconductors	21
1.B.7 Conclusion	23
II. OBJECTIVES OF INVESTIGATION	25
III. EXPERIMENTAL PROCEDURE	27
3.1 Preparation of Glass Specimens	27
3.2 Electrical Conductivity Measurements	28
3.2.1 Electrical Resistivity at Different Temperatures	28
3.2.2 Electrical Resistivity at Different Frequencies	31
3.3 Dielectric Measurements	32

CHAPTER		<u>Page</u>
IV.	RESULTS AND DISCUSSIONS	34
4.1	Electrical Conductivity at Different Temperatures	34
4.1.1	Bismuth Containing Glasses	34
4.1.2	Non-Bismuth Glasses	36
4.1.3	Conductivity Model in Amorphous Semiconductors	39
4.2	Electrical Conductivity at Different Frequencies at Room Temperature	41
4.3	Conformance to Some Recent Models	45
4.4	Dielectric Properties	47
V.	CONCLUSIONS	50
VI.	APPENDIX	52
	REFERENCES	63

I. INTRODUCTION

The unique properties of amorphous semiconductors and the advantages of producing them by means of thin-film process, which do not limit their size and make them adaptable to integration with other solid state technologies, have made these materials the base for a new area of Science and Technology. Applications of amorphous semiconductors either realized or anticipated include a very wide spectrum such as switching and memory devices, continuous dynode electron multipliers (channeltron), optical mass memories, phase contrast holograms, high-energy particle detectors, infrared lenses, ultrasonic delay lines. This is an impressive list in view of the fact that the scientific understanding of amorphous semiconductors to-day compares with that of crystalline semiconductors in the early 1950's.

The realization that thin films of certain amorphous semiconductors can exhibit a very fast and reversible conversion from a high-resistance to a low resistance state under the influence of an applied field is one reason for the very rapid growth of interest in amorphous materials - that took place in the last years of the decade 1960-70.

Therefore, a tremendous amount of interest was generated in the past few years to know the basic mechanism of conduction in amorphous semiconductors, which geared up the work of various researchers to come to a basic understanding of these materials.

Since the switching and memory effects are quite general to a large number of semiconducting glasses, these phenomena also need to be reviewed along with the semiconductivity in amorphous materials.

Hence, the following two aspects will be dealt with in this chapter with proper perspective:

- A. Switching Phenomena in Amorphous Materials,
- B. Semiconductivity in Amorphous Materials.

1.A Switching in Amorphous Solids:

1.A.1 Introduction:

Recently, there has been a growing interest in the study of electrical switching in amorphous materials. This switching effect comprises a sudden decrease of electrical resistivity by several orders of magnitude when a sufficiently high electric field is applied to the material. There are two types of switching possible - one is threshold switching where the switching material or the device (as it is called) jumps from a ~~high~~ resistance state (OFF-State) to ~~low~~ resistance state (ON-State) when the applied voltage exceeds a certain limit, characteristic of the material, called threshold voltage and the other one is memory switching which is shown coincidentally with the ON-State of the switching device, but stable at zero bias, i.e. the low resistance state (ON-State) is stable even after the external potential is removed.

The switching effects described in 1962^{1,2} were first demonstrated using the simple DC circuit shown in Figure 1a. The switching and memory effects reported upto date were shown by a large number of chalcogenide glasses¹⁻⁵ as well as amorphous elemental semiconductors^{6,7} and amorphous alloys⁸ outside of the glass forming region and oxide films⁹. Also this phenomenon has been observed in some oxide glass semiconductors¹⁰⁻¹³. Although switching occurs in a variety of other materials and even in liquid Se, S and Te alloys¹⁴ it is unlikely that the same mechanism is responsible in all cases.

1.A.2 General Device Characteristics:

Operation of a device under square wave pulsing¹ (the device being operated with a 10,000 ohm series resistor) has been found to produce an almost instantaneous switching to a low resistance condition and it appeared that the 'switching time' was faster than 1μ sec. The whole device² (Person Device) characteristic is summarised in Figure 1b. Where region 1 represents the ON or high conductivity state, region 2 the OFF or low conductivity state, and 3 represents the negative resistance state. Fast switching from 2 to 1 and 1 to 2 is achieved under nonconstant current conditions. If the critical current for the particular device is exceeded the memory state 1 will be observed. Under constant current conditions, the negative resistance state 3 is seen.

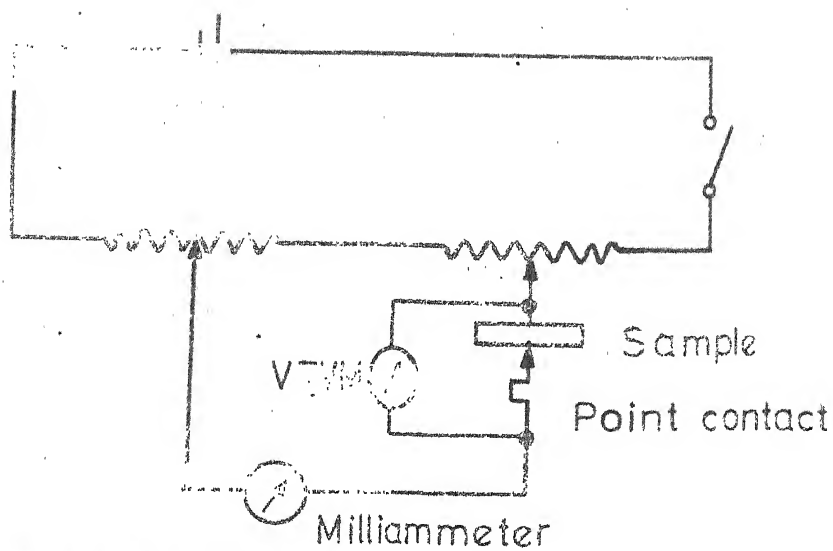


FIG. 1a. SAMPLE TESTING CIRCUIT.

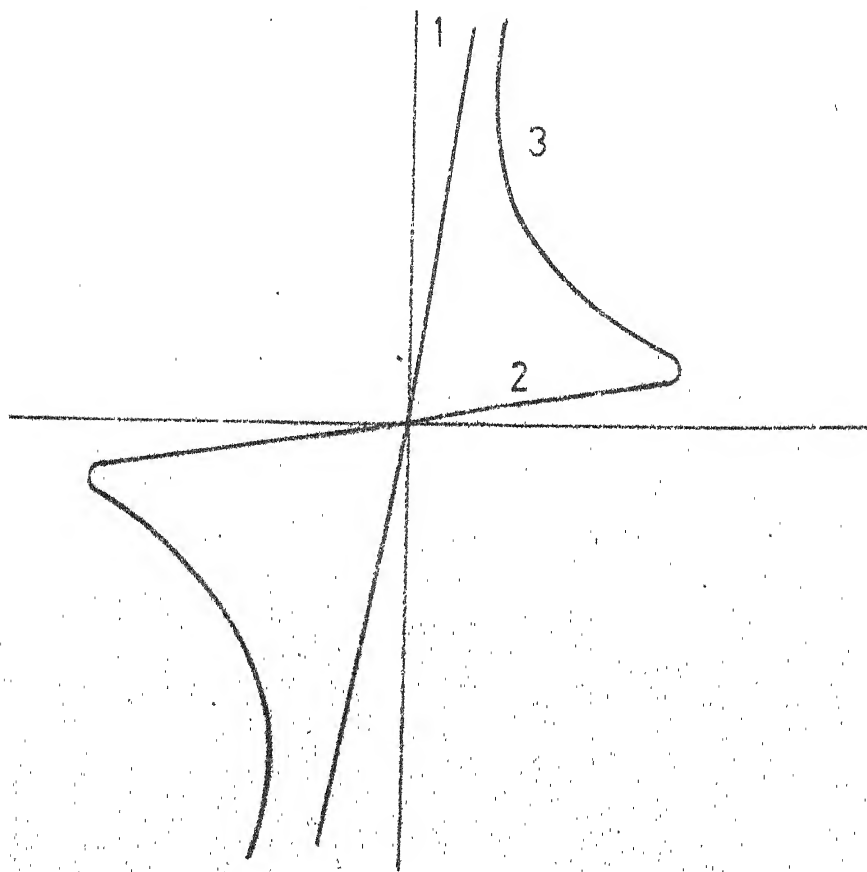


FIG. 1b. GENERAL DEVICE CHARACTERISTICS.

The same kind of switching and memory effects were reported in 1963 by Kolomiets and Lebedev³ for the $\text{TlAs}(\text{Se}, \text{Te})_2$ glass and they found that the 'switching time' depended on the magnitude of the applied voltage. The 'switching time' included both a 'delay time' and the 'actual time taken for the device to switch from high to low resistance. The delay time was found to increase with sample thickness. Ovshinsky⁴ has also reported a delay time of upto several micro-seconds before switching time to be 150 pSec., and notes that the delay time decreases as the magnitude of the voltage pulse is increased above the threshold voltage, while working on the system As-Te-Si-Ge. He confirms the previous reports¹ of ohmic behaviour at low fields in the OFF state, and the departure from ohmic behaviour at high fields just prior to switching. Ovshinsky also observes that in the ON State the current can be increased or decreased without significantly affecting the voltage drop across the device.

1.A.3 Threshold and Memory Switching:

Common to both types of devices is the switching process that occurs when the voltage drop exceeds a threshold voltage V_{th} or after a delay time t_D when a voltage pulse $V_P > V_{th}$ is applied. Once switching has commenced it proceeds very rapidly within a switching time $t_S < 10^{-10}$ s along the load line to the conducting branch of the

characteristic. In this conducting state the voltage drop is about $V_{th} \sim 1V$ and nearly independent of the current.

It has been found by Coward¹⁵ and Bosnell and Thomas¹⁶ that the threshold voltage necessary to switch virgin devices can be as large as 10 times that for a subsequent switching and one to a thousand operations may be necessary before a stable threshold is reached. This process is temperature sensitive¹⁶. On a number of compositions, the threshold voltage becomes equal to the holding voltage at approximately the glass transition temperature, T_g , as indicated by Thomas et. al.¹⁷. The memory state is realized by passing current through the device in the ON state so that a critical current is exceeded. This critical current varies depending upon the composition of the glass being used, the device thickness, the temperature, and perhaps other parameters. The device can be made to switch back from the memory state to the high resistance OFF state by passing through it a pulse of current again greater than a particular critical value for composition and geometry, and having a sharp tailing edge. The principal difference¹⁸ between the two devices is the existence in the threshold switch of a holding current value I_h below which the conducting state cannot be maintained, i.e. when the current falls below this value the threshold switch returns to its original high-resistance OFF state. In contrast, the memory switch

retains its conductance state even when the current approaches and reaches zero or is reversed.

In a memory device, as the pulse width is increased, that is, the power input in the ON state of the device is increased, 'lock-on' into the memory state occurs. The memory switch retains its conductance state only after it has been kept in this state for a sufficient period of time, the lock-on time t_{LO} , to 'set' the memory state. If the set pulse V_P is shorter than $t_D + t_{LO}$ then the memory switch reverts back to its high resistance state as if it were a threshold switch. However, after lock-on the memory switch is in permanent conductive state. The lock-on period represents the time needed to allow the material in the current channel to devitrify. The lock-on time is variable for the same memory device from operation to operation.¹⁹

It is generally agreed that a crystalline filament is formed which is broken up by a high current 'reset' pulse which returns the device to its OFF state.

An additional state which can be realized in these devices consists of a negative resistance condition. This can be obtained by operating the device using a constant current power supply. Alternatively a series resistor having a very large value compared to the OFF resistance of the device may also be used to approximate constant current conditions.

1.A.4 Mechanisms of Switching:

There are two schools of thought on the basic mechanism of switching - one is thermal mechanism put forward by Pearson²⁰, Boer²¹, and Kaplan and Adler²² and the second is electronic mechanism by Henisch and Pryor²³.

1.A.4.1 Thermal Mechanism:

The thermal mechanism suggests the existence of memory effect is explainable by means of a phase change process. It seems reasonable to propose that the passage of large currents in the ON state of the switch result in enough Joule heating to allow phase changes to occur. If new phases, which are probably crystalline, are of high conductivity and extend continuously between the electrodes, then they would form a conducting path which would be stable at zero bias. The passage of a critically large current pulse in the memory state would result in the fusion of 'hot-spots' along this path. If the current ceased abruptly, these fused regions would be quenched to the glassy state. Since this has a high resistivity the device would then be OFF. Slow cessation of current flow would result in slow cooling of the fused 'hot-spots' and recrystallization or phase separation to reform the continuous conducting path. Thus, under these conditions the device would remain in the memory state.

Recent work by Bagley and Bair²⁴ supports this mechanism. They observed a general correlation between ease of attaining the memory state and fast crystallization kinetics, adding further evidence in support of the thermal mechanism of phase change of memory operation.

Further experiments by Peason and Miller²⁵ have indicated more support for the filamentary conduction hypothesis. Recent work by Bosnell and Thomas²⁶ also supports this mechanism. It is now generally agreed that the electrical memory effect is caused by formation of a conductive crystal filament in the glass.²⁷⁻³⁰ But in Mott's³¹ view there is still some uncertainty in these treatments about the filament width and its dependence on current.

1.A.4.2 Electronic Models:

The major alternative explanation of the switching action is the class of electronic models typified by Henisch and Pryor²³ and Van Roosbroeck³². The experiments reported²³ show that ovonic threshold switching is essentially a non-thermal process. The conclusion is that one or more electronic mechanisms are at work, and this is further reinforced by the results of recent observation by Ovshinsky et.al.³³ on ovonic memory switching.

The electronic models suggest that a double injection space charge process is taking place within the material.

A neutral plasma, thus produced, creates an instability which is propagated through the material resulting in a voltage drop across the device and the observed S-shaped negative resistance in the switch characteristic. Hence the potential breakdown mechanism is stabilised. Electronic mechanisms may be polar or non-polar, and the experimental results show the both types prevail. For some chalcogenide glasses there is room temperature evidence for space-charge controlled conduction process as indicated by Kolomiets³⁴. A space charge model previously proposed by Henisch et.al.³⁵ and Henisch et.al.³⁶ envisage polarisation and space charge reveals in the course of switching.

A number of electronic processes have been proposed so far, e.g., space charge overlap as suggested by Henisch³⁷, field assisted hopping by Fritzsche³⁸ and impact avalanche formation as proposed by Hindley³⁹. So many other workers have confirmed the validity of electronic models with some success.

1.A.5 Switching in Oxide Glasses:

The discussion so far was centred mostly round chalcogenide glasses. In recent years there has been some investigation of switching effects in some oxide glass semiconductors¹⁰⁻¹³. Drake et.al.¹⁰ have observed memory phenomena in oxide glasses containing a large proportion of oxides of certain variable valence transition metal ions. Bishay et.al.¹¹

have observed the same phenomena in calcium-borate glasses containing iron oxide and confirmed the filamentary type of conduction in the direction of the applied field. Chakravorty¹² observed such memory switching effects induced in some phase-separated glasses by ion-exchange treatments ($\text{Na}^+ \rightleftharpoons \text{Ag}^+$) and subsequent reduction by hydrogen, the glass composition being $10 \text{ Na}_2\text{O} \cdot 18\text{B}_2\text{O}_3 \cdot 64 \text{ SiO}_2 \cdot 8 \text{ Bi}_2\text{O}_3$ (Mole %). The specimen studied by Chakravorty¹³ has a resistance of $8 \times 10^9 \text{ ohm}$ (OFF state) and at about 3 volts it switches onto a resistance of $2 \times 10^3 \text{ ohm}$ (ON state) which is preserved even when the applied voltage across it is removed. The specimen can be reverted to the OFF-state using a 20-V pulse of 10 μsec width.

The ON-state conduction in the glass specimen studied by Chakravorty¹³ is proven to be filamentary in nature. The switching effects observed by him in this glass has been associated with micro-structural characteristics.

1.A.6 Conclusion:

The central question of whether the switching mechanism of these devices depends upon phase changes or upon electronic effects must at present be quite speculative. Certainly the speed at which phase changes can travel is adequate to explain the switching speeds which have been observed. However, this does not mean that the phase change mechanism

of switching is definitely proven. The same also applies to speculations on electronic mechanism of switching operation. On the basis of the results so far published, it can be said that thermal run-away in some systems is only stabilised if phase separation occurs. There are perhaps compositions where either a purely electronic or thermal mechanism is feasible but so far there is little evidence for this. But the first fire processes seem always to occur. It is difficult to see a unique solution to all the observed cases at present.

Therefore the whole matter is in need of further study. As the detailed properties of the switching devices become known, the interpretational options become more restricted and the 'switching mechanism' correspondingly clearer.

1.B Semiconductivity in Amorphous Materials:

1.B.1 Introduction:

Ten years ago our theoretical understanding of electrons in non-crystalline materials was rudimentary. The classification of materials into metals, semiconductors, and insulators was based on band theory, and band theory starts from the assumption that the material is crystalline. Interests on the electronic behaviour of non-crystalline solids started growing to throw some light on this aspect from a different angle. The idea that the property like electrical conduction is due to the movement of electrons was supposed to be based on a

strong footing of scientific knowledge. A milestone in the development of the subject was Ziman's⁴⁰ quantitative explanation of the electrical properties of liquid metals, put forward in 1960. This was a weak-interaction theory, the effect of each atom being treated as small. The success of this theory prompted investigations of what happens when the interaction is large, as it must be when an energy gap exists. The keys to our present understanding have been the principle of Ioffe and Regel⁴¹ that the mean free path cannot be less than the distance between atoms, and the concept of localization introduced by Anderson⁴² in 1958.

It was first emphasized by Ioffe and Regel⁴¹ that when the interaction of the carrier with atoms is sufficiently strong, something new ought to happen. It was first conjectured by Gubanov⁴³ in 1963 and by Banyai⁴⁴ in 1964 that near the edges of conduction or valence bands in most non-crystalline materials the states are localised, and the concept of localization plays a great role in understanding the basic mechanism of conduction in amorphous solids.

1.B.2 Anderson's Localization Theory:

The concept of localized states can be approached by considering the d.c. conductivity $[\sigma_E(0)]$ of a system with states filled upto a limiting value E_F (Fermi Energy). At low temperatures two limiting cases have been distinguished:

(a) Situations in which the conductivity is determined by the properties of electrons with energies near E_F . This is so in metals, crystalline or liquid; it is also the case in impurity conduction at low temperatures whether or not the motion of electrons is by thermally activated hopping.

(b) Situations where the mobility of electrons with energies near the Fermi energy E_F is zero or negligibly small, or in which the density of states $N(E)$ is Zero there. The current is carried by excited electrons, as in an intrinsic semiconductor, or as in an extrinsic semiconductor if impurity conduction is absent.

It is known that electrons can be described by wave functions each having a fairly well-defined wave number K , the uncertainty in that being ΔK . In the case of strong interaction a density of states $N(E)$ that is a continuous function of E remains a valid concept, if and only if $\Delta K/K \sim 1$ (or localization) in the regions where the deviation of $N(E)$ from the free-electron value is large. The form of $N(E)$ vs. E curve is shown in Figure 2a for an intrinsic semiconductor.

There is nothing unfamiliar about the concept of localised states; they are simply 'traps', and the most direct evidence for their existence in amorphous materials is provided by measurements of the transit time for injected carriers; if this shows an activation energy, a trap-limited mobility can be inferred.

In case (a), the concept for amorphous materials is that a continuous density of states, $N(E)$, can exist in which for a range of energies $N(E)$ is finite but the states are all traps, or in other words 'localized', and for which the mobility of an electron with such an energy is zero at $T = 0$, even though the wave functions of neighbouring states overlap. For these energies $\sigma_E(0)$ also vanishes. The vanishing of $\sigma_E(0)$ can serve as a definition of localization for electrons with energy E , other definitions of localised states are possible. One is that any eigen-functions that do not decay exponentially are so rare as to contribute a term $\sigma_E(0)$ that tends to zero when the number of atoms (N) tends to infinity. Or, alternatively it can be said, following Anderson, that states are localised if an electron, with energy $E \pm \Delta E$ placed in a volume l^3 , large enough to satisfy the uncertainty principle, will not diffuse away. It is now believed that all the definitions are equivalent.

In case (b), that of an intrinsic semiconductor, the concept of localisation is important too. It is found that for non-localised states $\sigma_E(0)$ can be interpreted as $eN(E)/KT\mu$ where μ is the mobility for carriers with energy E , always with neglect of the effects of interaction with phonons. If states are localised, μ vanishes at $T = 0$. At finite temperatures the mobility is essentially due to interaction with phonons and is several orders of magnitude smaller than for non-localised (extended) states.

It is said that states with energy E are localised if $\langle \sigma_E(0) \rangle = 0$, where $\langle \sigma_E(0) \rangle$ is average of $\sigma_E(0)$ over all possible configurations of the ensemble.

For an assembly of N atoms, a range of electron energies may exist such that the number of configuration for which σ does not vanish tends to zero as $N \rightarrow \infty$. Thus the definition of localization is that, for a Fermi gas of non-interacting electrons with Fermi energy E ,

$$\lim_{n \rightarrow \infty} \langle \sigma_E(0) \rangle = 0.$$

The first phenomenon for which this was generally recognized was impurity-conduction in doped and compensated semiconductors, which was first fully understood in the early 1960's. The centres in these materials are located at random positions, and in addition there is a random potential at each centre. Our understanding of localization in this case derives from Anderson's theory, which is central to our theme.

In impurity-conduction, each time an electron moves from one centre to another, it emits or absorbs a phonon; processes in which it absorbs a phonon are rate determining, and in consequence the conductivity contains an activation energy and tends to zero at low temperatures. This form of charge transfer is called 'thermally activated hopping', or just hopping. Hopping is also responsible for an a.c.

conductivity $\sigma(\omega)$ at frequency ω proportional to $\omega^{0.8}$.

In this process, an electron hops between pairs of localized states, absorbing or emitting a phonon each time.

1.B.3 Mott's Hypotheses of Conduction:

First of all, it is emphasized⁴⁵ that the density of states remains a valid concept for non-crystalline as for crystalline materials and can be determined by techniques such as photo-emissions. The hypotheses are as follows:

(a) The main factors determining the density of states for a given material are the first coordination number and the interatomic distance. Thus if the former is unchanged, no major change in the density of states is likely except that due to changes in the specific volume. Coordination numbers higher than the first will of course influence the density of states to some extent. In Ge, the third coordination number is different in the crystalline and amorphous forms: there is an effect of this on density of states. In crystalline Te higher coordination strongly affect the magnitude of the smallest energy gap and this is very much changed in amorphous form.

(b) The wave number K is not a good quantum number for electron states in many non-crystalline materials. Either the mean free path is so short that $\Delta K/K \sim 1$, or else the states are localized. Neither is true near the Fermi energy of most

liquid metals, where the density of states is high, nor at the bottom of the conduction band of liquid rare gases where the wave functions are S-like.

(c) In semiconductors that do not have S-like conduction and valence bands, localized states occur at the band extremities in the amorphous phase. Energy values E_c and E_v separate these localised states from non-localized (extended) states, and there is a drop by a factor ~ 1000 in the mobility as the energy crosses these values (the mobility shoulders). The energy difference ($E_c - E_v$) defines a mobility gap E_g .
[2.6 (i) and (ii)]

Although it seems clear that the Fermi level lies near the middle of the band gap, it is uncertain whether for a given amorphous semiconductor the conductivity is intrinsic or extrinsic. By intrinsic we mean that the position of the Fermi level is controlled by the densities of states in the conduction and valence bands. In such a situation the Fermi level moves (linearly) with temperature in such a way as to keep the total concentration of excited electrons equal to that of holes.

It should be noted however that even in this case, if the range of localized states at the edge of, say, the valence band is smaller than at the conduction band, the number of holes excited below E_v will exceed the number of electrons excited above E_c and the material can behave as a p-type semiconductor.

Cohen, Fritzsche and Ovshinsky⁴⁶ have suggested that in certain glasses the density of states is as shown in Figure 2b(iii) the conduction and valence bands have tails of localised states sufficiently extensive to overlap near the centre of the mobility gap. Electrons from states at the top of the valence band are transferred into states at the bottom of the conduction band, ensuring that the Fermi level lies in the region of overlap.

An alternative model suggested by Davis and Mott⁴⁷ is shown in Fig. 2b(iv). A fairly narrow (< 0.1 eV) band of localised states is assumed to exist near the centre of the gap, of sufficiently high density to effectively pin the Fermi energy over a wide temperature range. Thus conduction is extrinsic rather than intrinsic. The origin of the states is speculative, but they could conceivably arise from some specific defect characteristic of the material, for example dangling bonds, interstitials etc., the number of which will be dependent on the conditions of sample preparation and subsequent annealing treatments. This model seems more compatible with the high transparency shown by many glasses as photon energies below the fundamental absorption edge.

Evidence for a fairly high density of states of the Fermi energy comes from a.c. conductivity and other measurements that surface (Schottky) barriers are very narrow in amorphous semiconductors. It should be pointed out that at present there

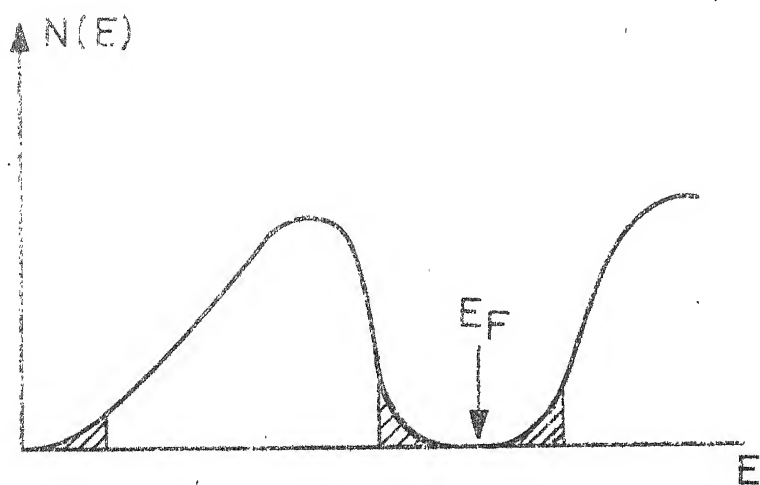


FIG. 2a. DENSITY OF STATES IN NON-CRYSTALLINE MATERIALS (Schematic). E_F IS THE FERMI ENERGY AT ABSOLUTE ZERO OF TEMPERATURE ; LOCALISED STATES ARE SHADED.

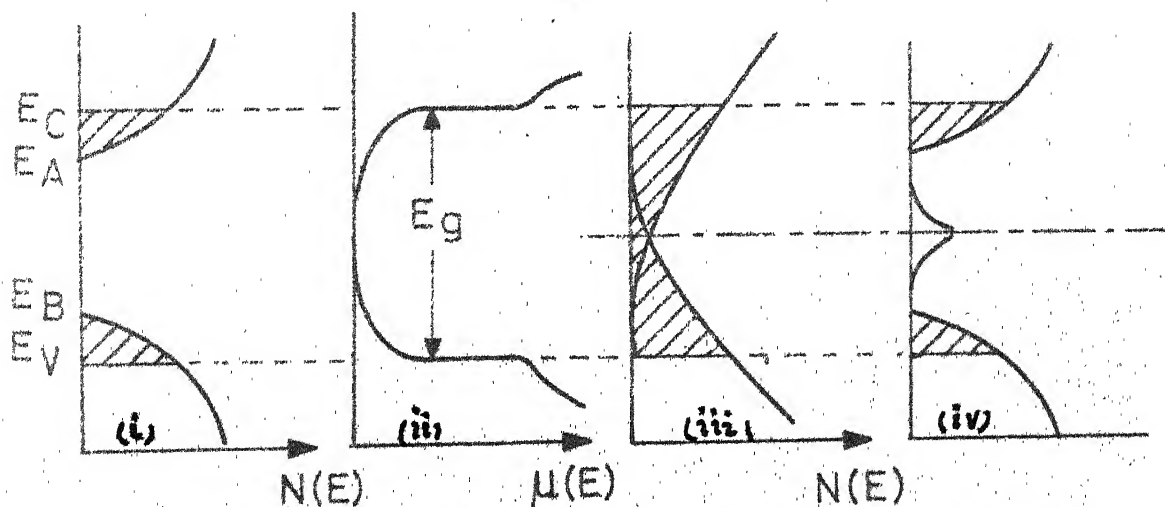


FIG. 2b. DENSITY OF STATES AND MOBILITY AS FUN OF ENERGY IN AMORPHOUS SEMICONDUCTOR

is no definite evidence for the existence of such states from optical absorption or photo-emission measurements, although in amorphous Ge there is some evidence for absorption due to defects.

1.B.4 A Comparison between Crystalline and Amorphous Semiconductors:

The characteristic differences between amorphous and crystalline semiconductors that appear particularly important for understanding a variety of applications and phenomena need some emphasis here.

Perhaps the most striking feature of amorphous as compared to crystalline semiconductors is that addition of atoms with valencies different from that of the host does not in general greatly affect the conductivity, i.e. they can not easily be doped. The generally accepted explanation is that the disordered structure, including impurities accommodates itself so that all the electrons are taken up in bonds. There is evidence that structural defects play a more effective role than do impurities in controlling the conductivity of amorphous semiconductors. A second and equally important observation is that, near room temperature for most of the materials with which we are concerned, the activation energy for electrical conduction is approximately equal to one half of the Photon energy corresponding to the onset of strong optical absorption.

Furthermore, in cases where a comparison is possible, there is good correspondence between these energies and those occurring in an intrinsic crystalline sample of the same material.

The differences from rather than the similarities to crystal turn out to be the exciting attributes of amorphous semiconductors. Two important aspects of crystalline semiconductors are missing in their vitreous counterparts. The first is the possibility of changing by impurity doping the conductivity of crystalline semiconductors by many orders of magnitude. The second is the possibility of forming p-n junctions by choosing different doping elements.

The reason for this is that in a crystalline semiconductor a donor or acceptor doping element acts as such because it is forced to take the place of a crystalline host atom and hence has either an excess or a deficiency of a valence electron. In an amorphous semiconductor, on the other hand, the local order is not forced to be same everywhere; as a result each atom can satisfy its valency requirements and hence does not act as a conventional donor or acceptor as in crystalline semiconductors. This different response to chemical doping explains some characteristics that have important consequences for devices.

1.B.5 Some Characteristics of Amorphous Semiconductors:

- 1) Amorphous semiconductors behave similarly to intrinsic semiconductors. Their low conductivity enables one to observe high-field effects without excess heating.
- 2) Contacts to many amorphous semiconductors are non rectifying and non-blocking essentially because these materials behave like intrinsic semiconductors. The majority carrier current equilibrate via generation and recombination with relatively large minority current in the barrier region.
- 3) A very important distinction⁴⁸ concerns the chemical bonding. In the chalcogenide semiconductors the unshared p-electrons of the Group VI elements form the valence band and the antibonding state the conduction band.
- 4) A disordered semiconductor can^{be}/in several structural states. In many disordered semiconductor it is possible to control the short range order parameter and thereby achieve drastic changes in the physical properties of these materials, including forcing new coordination numbers for elements.

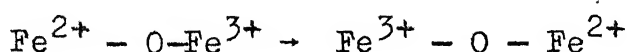
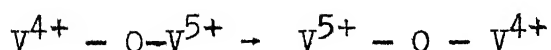
1.B.6 Classification and Description About Amorphous Semiconductors:

The number of possible amorphous semiconductors is immense because the structural disorder allows the existence in a metastable state of non-stoichiometric compositions and mixtures that have no crystalline equivalent.

Semiconducting glasses can be classified into two groups:

- (a) Semiconducting oxide glasses,
- (b) Semiconducting chalcogenide glasses.

Both these groups have their individual characteristics. Interest and activity in the field of electronic conduction in glassy materials increased since 1954 when Devton, Rawson and Stanvorth⁴⁹ found that glasses in the system $P_2O_5 - V_2O_5$ exhibited bulk electronic conduction. Various other oxide glasses have been studied by various workers after that. A range of vanadate - phosphate, vanadate - germanate glasses have been studied by Mackenzie^{50,51}, Han-blen et.al.⁵², Munakata^{53,54}, Bayuton et.al.⁵⁵, and Ioffe and Regel⁵⁶. Some Germanate-Vanadate - Phosphate glasses have been studied by Janakirama Rao⁵⁷. Iron-oxide based glasses have been studied by Hansen⁵⁸ and Mackenzie⁵⁹. The conduction in most of these glasses was pictured to be the transfer of an electron (and/or hole) between ions of the same transition metal in different valence states, e.g.



(b) The d.c. conductivity of most chalcogenide glasses near room temperature obeys the relation $\sigma = C \exp (-E/KT)$, where E varies from 0.3 eV to 1 eV. There are different

binary and ternary compositions of chalcogenides studied by different workers. The following systems have been studied so far: Ge-Te system by Tsu, Howard and Esaki⁶⁰, $\text{As}_2\text{Te} \cdot \text{Tl}_2\text{Se}$ glass by Andriesh and Kolomiets⁶¹, As_2Te_3 by Waiser and Brodsky⁶², $4\text{As}_2\text{Te}_3 \cdot \text{As}_2\text{Se}_3$ by Uphoff and Healey⁶³, $\text{As}_2\text{Se}_2 \cdot \text{Tl}_2\text{Se}$ by Kolomiets⁶⁴, $3\text{As}_2\text{Se}_3 \cdot 2\text{Sb}_2\text{Se}_3$ by Platakis et.al.⁶⁵, As_2Se_2 by Edmond⁶⁶ and As_2S_3 by Edmond⁶⁷, Owen and Robertson⁶⁸ and Polanco and Roberts⁶⁹.

The values of C has come in the range $10^3 - 10^4 \text{ ohm}^{-1} \text{ cm}^{-1}$, indicating conduction in extended states. Much lower values have been observed in some other materials and for these it has been suggested that conduction is predominantly by carriers hopping between localised states at the band edge. There is a variation of E and C observed in various binary and ternary systems as a function of composition.

1.B.7 Conclusion:

Different mechanisms have been proposed so far on electrical behaviour of amorphous solids. The controversy between Cohen's hypotheses and Mott's theory, concerning the peak in the density of localised states has arisen because of the conflict between the density of the 'gap states' as predicted from conductivity measurements and from optical absorption experiments. The data so far published seem to support Mott's theory.

Although the conception of density of states remains valid for both crystalline and non-crystalline materials, mathematical methods have yet to be developed for calculating the density of states for real non-crystalline materials - so that a clear picture can be obtained to add to our knowledge about amorphous semiconductors.

II. OBJECTIVES OF INVESTIGATION

It has been observed before that $\text{Na}_2\text{O}-\text{B}_2\text{O}_3 - \text{SiO}_2-\text{Bi}_2\text{O}_3$ glass shows memory switching effects after ion-exchange ($\text{Na}^+ \rightleftharpoons \text{Ag}^+$) and reduction in hydrogen. The question arises as to whether the base glass is semiconducting and whether Bismuth induces some semiconducting characteristics in these glasses, or the presence of silver, either in metallic or ionic state, is necessary for getting this semiconducting behaviour.

Another aspect of the problem which needs investigation is that if the base glass is semiconducting, it is important to know the basic mechanism of electron transport in these materials and to make an assessment of the influence of the ionic and electronic transport on the overall conductivity characteristics of the material, since $\text{Na}_2\text{O}-\text{B}_2\text{O}_3-\text{SiO}_2$ glass is known to give ionic conductivity.

The present investigation was initiated to study the following:

(i) A.C. conductivity of the bulk glasses (not ion-exchanged) containing Bismuth as a function of temperature at 1.0 kc/s to distinguish the ionic and electronic parts of conduction separately,

- (ii) A.C. conductivity of the bulk glasses containing no bismuth to establish the ionic part and to indicate the effect of Bismuth,
- (iii) A.C. conductivity of the bulk glasses as a function of frequency at room temperature to understand the mechanism of electron transport,
- (v) The real and imaginary parts of dielectric permittivity as a function of frequency at different temperatures. to investigate the contribution of electron transport to dielectric properties,
- (vi) To make these studies as a function of composition.

The composition of glasses studied belong to the following systems;

- (i) $\text{Na}_2\text{O} - \text{B}_2\text{O}_3 - \text{SiO}_2 - \text{Bi}_2\text{O}_3$
- (ii) $\text{Na}_2\text{O} - \text{B}_2\text{O}_3 - \text{SiO}_2$
- (iii) $\text{Na}_2\text{O} - \text{CaO} - \text{SiO}_2 - \text{Bi}_2\text{O}_3$
- (iv) $\text{Na}_2\text{O} - \text{CaO} - \text{SiO}_2$

III. EXPERIMENTAL PROCEDURE

3.1 Preparation of Glass Specimens:

The composition of glasses studied belong to the following systems:

- (i) $\text{SiO}_2 - \text{B}_2\text{O}_3 - \text{Na}_2\text{O} - \text{BiO}_{2.3}$
- (ii) $\text{SiO}_2 - \text{B}_2\text{O}_3 - \text{Na}_2\text{O}$
- (iii) $\text{SiO}_2 - \text{CaO} - \text{Na}_2\text{O} - \text{Bi}_2\text{O}_3$
- (iv) $\text{SiO}_2 - \text{CaO} - \text{Na}_2\text{O}$

The exact compositions of the glasses in mole % are shown in Table 1.

The glasses were prepared from reagent grade chemicals. Sodium was introduced as sodium carbonate, calcium as calcium carbonate, boric oxide as boric acid and all other components as their respective oxides. The glasses were melted in sintered alumina crucibles in an electrically heated furnace, with silicon carbide heating elements, at temperatures ranging from 1200° to 1300°C . Molten glass was poured in round (≈ 1 inch dia.) aluminium moulds, placed on a thick sheet of aluminium. The thickness of the cast pieces were 4 to 6 mm; which were then removed to a canthal-wire wound furnace for annealing. The annealing time and temperature was different for different glass compositions. After annealing the glass pieces were polished in silicon carbide grit of different

mesh sizes ranging from 120 to 600. The polished specimens having uniform thickness were then stored in a dessiccator. The specimens for electrical resistivity and dielectric measurements, in the form of discs. 25 mm. dia and 2 to 3.5 mm. thick, were cast from the same melt. The thermal history of glass-melting was almost same for all the glass compositions studied.

3.2 Electrical Conductivity Measurements:

3.2.1 Electrical Resistivity at Different Temperatures:

The electrical resistivity of the glass specimens were measured as a function of temperature at 1.0 Kc/s . The experimental set-up made for this purpose is clearly shown in Figure 3.

The experiments were done with a capacitance Bridge of General Radio Company (Type 716-C) above a resistance value of 10^7 ohm and below this value a Mag-ohm Bridge (Type 1615A) was successfully used keeping the frequency at 1.0 Kc/s.

The accessories used in conjunction with the capacitance Bridge are the following:

- (i) R-C oscillator unit, range 20 c/s to 500 kc/s,
Type No. 1210-C.
- (ii) Regulated power supply, Type 1267-AQ18.
- (iii) Tuned amplifier and Null Detector, Type 1232-A.

- (iv) A pair of Batteries of 12 volts.
- (v) Polystyrene Decade Capacitor, Type 1419-B, with a setting of 200 p Farad during the time of measurements.

All these instruments are from General Radio Co.(USA).

While measuring by Capacitance Bridge the capacitance and dissipation values were first taken without the specimen (i.e. C_1 and D_1), just by raising the upper cell, M_1 , one inch above the specimen and holding it with a clamp. Secondly these values were taken with specimen in touch with both the cells M_1 and M_2 (i.e. C_2 and D_2). The temperature was kept constant with an accuracy of $\pm 1^\circ\text{C}$. The furnace temperature was controlled by a API controller, the chromel-alumel thermo-couple was introduced from the top. Another chromel-alumel thermo-couple was inserted from the bottom of the furnace tube and was kept at 1 mm. apart from the specimen. The specimen temperature was thus correctly measured with a potentiometer and ice was used in the cold-junction.

The following formulae were used, from circuit diagram of the instrument, for calculating the resistance values:

$$R = \frac{1}{\omega \cdot C_x \cdot D_x} \quad (1)$$

where $\omega = 2\pi f$

f = frequency in cycles = 1000 c/s (in this case)

$$C_x = \text{capacitance of the sample} = (C_1 - C_2) = \Delta C.$$

$$D_x = \frac{C_1 \times (D_2 - D_1) \times 0.01 \times M \times f_0}{\Delta C}$$

In this particular case M was equal to 1.0 and f_0 was always kept at 1.0 kc/s.

For Meg-ohm Bridge the resistance values were directly read from the dial. The resistivity values were calculated by multiplying the resistance values with the factor A/l expressed in cm., where A is the area of the top electrode surface in sq.cm. and l is the exact thickness of the specimen in cm. without electrode thickness, since we know that

$$\rho = R. (A/l) \quad (2)$$

where R = Resistance of the specimen, and

ρ = Resistivity of the specimens.

The values of the factor (A/l) for different glass specimens used for different experiments are shown in Table 2.

The electrode used for this experiment was aluminium. The aluminium was vapour deposited by putting a stainless steel ring on one surface of the specimen. The upper electrode area was having a diameter equal to the inner diameter of the ring, the bottom surface of the specimen was covered fully. On the top surface, an annular concentric portion remained undeposited leaving a circular deposited area outside, which facilitated putting the 'Guard-ring' in the circuit,

since the electrical resistivity measurement was done with the Guard-ring to prevent surface conduction. The width of the annular space left undeposited was equal to the width of the S.S. ring.

3.2.2 Electrical Resistivity at Different Frequencies:

The electrical resistivity of the glass specimens (only glass Nos. 1 and 3) were measured as a function of frequency at room temperature (20°C).

The resistivity was first measured by the capacitance Bridge following the same principle as mentioned before and using a standard sample holder upto a frequency of 100.0 kc/s.

Secondly it was measured by a Boonton Q-meter (Type-260, A) of Boonton Radio Co. (USA) above 100.0 kc/s using different standard inductors (Type 103A) for different frequency ranges.

The resistance values for the lower frequency region were calculated using equation (1) at different frequencies. The resistance values for the higher frequency region were measured in the Boonton Q-meter using a Aluminium connector placed on two terminals of the instrument. The capacitance (C) and Q-values were first measured by keeping the sample in touch with the connector (i.e. C_2 and Q_2 values) and secondly without the sample, leaving an air gap between the two connectors (i.e. C_1 and Q_1) values at each frequency. The measurements were repeated at each frequency to see the fluctuations which

were almost nil in this case. The following formula was used to calculate the resistance values at different frequencies:

$$R = \frac{Q_1 \times Q_2}{\omega \times C_1 \times \Delta Q} \quad (3)$$

where, $\omega = 2\pi f$

f = frequency in cycles

$$\Delta Q = (Q_1 - Q_2)$$

The resistivity values were calculated by multiplying the resistance values with the factor (A/l) in both the cases, using equation (2). The electrode material used in this experiment was silver which were applied on the surfaces of the specimens with a brush; keeping the correct consistency of the paste, used for this purpose, with a standard 'thinner'. The specimens were dried in a Lab.-drier at 70°C for 1/2 hour.

3.3 Dielectric Measurements:

The dielectric measurements were done with the glass No. 1 only, at different frequencies and at different temperatures. The same experimental set-up, as in conductivity experiment, was used for this purpose, as shown in Figure 3.

The C_1 and D_1 values were taken without the sample and the C_2 and D_2 values were taken with the sample, using the same 'capacitance Bridge'. The following formulae were used to calculate the dielectric constants:

$$(i) \quad \epsilon' = \frac{\cancel{8.854} \times \cancel{1}}{\cancel{A}} = \frac{C_x \cdot l}{\epsilon_0 \cdot A} \quad (4)$$

where ϵ' = real part of the dielectric constant

ϵ_0 = a constant = 8.854

l = thickness of the specimen in meters

A = Area of the electrode area in sq. meters.

$$(ii) \quad \epsilon'' = \epsilon' \tan \delta \quad (5)$$

$$\text{where } \tan \delta = D_x = \frac{C_1 \times (D_2 - D_1) \times 0.01 \times M \times f_0}{\Delta C},$$

the terms have got their usual meaning as before.

IV RESULTS AND DISCUSSIONS

4.1 Electrical Conductivity at Different Temperatures:

4.1.1 Bismuth Containing Glasses:

The results of the conductivity experiment with temperature for glass nos. 1 and 3 are shown in Tables 3 and 5.

Since it was not known initially whether the glass has any electronic contribution to conductivity or not the following formula was used to describe the behaviour of resistivity with temperature:

$$\rho = \rho_0 T \exp (E/kT) \quad (4.1)$$

where ρ = Resistivity of the specimen,

ρ_0 = A pre-exponential constant

E = Activation energy for conduction process

K = Boltzman's constant

T = Temperature in absolute scale

This equation is generally used to explain the change of ionic conductivity with temperature. The plot of $\log (\rho/T)$ vs. $1/T$ is shown in Figures 4 and 5 for glass Nos. 1 and 3. The slopes of these plots yield the activation energies for conduction in different glasses.

For glass No. 1 the important feature of this plot (Figure -4) is that there is a change of slope at a temperature

of 232°C . The activation energies were calculated to be 30.8 kcal/mole and 1.4 kcal/mole, respectively above and below that temperature, from two distinct straight lines as shown in Figure 4.

The same type of behaviour is also observed in glass No. 3, where the change of slope (Figure 5) comes at around 184°C . From two distinct straight lines, above and below this particular temperature, the activation energies were calculated to be 23.0 kcal/mole and 1.3 kcal/mole respectively. For glass Nos. 1 and 3 the breaking points i.e. the temperatures at which the slopes of the curves change, occur at 232°C and 184°C below which the activation energies, from the slopes of the $\log (\sigma/T)$ vs. $1/T$ plots, seem to be quite low for ionic conduction in these glasses. Such low activation energy values have been ascribed to electronic conduction in oxide glasses by many investigators. Therefore, it has been thought that there is a mixed effect of ionic and electronic conduction on the overall conductivity of these glass specimens, since above those breaking points, the activation energies, i.e. 30.8 kcal/mole and 23.0 kcal/mole for glass Nos. 1 and 3, are quite reasonable for ionic conduction. It should be noted that soda-content of glass Nos. 1 and 3 are 10 and 25 mole % respectively and it is quite possible that above those temperatures the ionic conductivity will be predominant due to the field-induced drift of sodium ions along with thermal activation.

The glass Nos. 1 and 3 contain 8 and 10 mole % Bismuth oxide respectively and it is seen that the conductivity is higher in glass No. 3 than in Glass No. 1 showing the effect of Bismuth in conduction below the breaking points, since it is believed that Bismuth is responsible for electronic conduction in this low temperature region. It is also observed above these breaking points since the soda content is higher in glass No. 3 than in glass No. 1. Because the migration of the sodium ions through the glass structure can be ascribed to the ionic conduction in these glasses.

It can be said from the data of activation energies for ionic conduction that the glass structure is more rigid in glass No. 1 because of the large number of network-formers (i.e. silicate and borate) and also the amount of silica is more in glass No. 1 than in 3. Therefore the idea that the stiffening index is more in glass No. 1 than in 3, as is shown up by a higher value of activation energy in this glass, seems to be consistent. However, at this stage it is only an optimistic approximation about the structure of these glasses. The effect of bismuth on electronic conduction in these glasses was studied by carrying out conductivity experiments on two non-bismuth glasses of the above two systems.

4.1.2 Non-Bismuth Glasses:

(i) In glass no. 1 the bismuth oxide was replaced by boric oxide and a non-bismuth glass was prepared (i.e. glass no. 2).

The results of the conductivity experiment with temperature on this glass is shown in Table 4. Since there was no bismuth present in this glass and since this glass was assumed to show ionic conduction, the equation (4.1) was used to describe the behaviour of conduction in this glass. The plot of $\log (\sigma/T)$ vs. $1/T$, is shown in Figure 4, which gives a straight line. The activation energy from the slope of the curve was calculated to be 35.8 kcal/mole which is consistent with the values reported before for this type of glasses. There is no change of slope even in the low temperature region, i.e. the glass shows a straight line behaviour all through the temperature range studied in this case, thereby indicating that Bismuth responsible for electronic conduction and consequently a change of slope, in the $\log (\sigma/T)$ vs. $1/T$ plot after a certain temperature while bismuth is put in this glass system (i.e. glass no. 1). The activation energy in glass no. 2 is slightly higher than in glass no. 1 which is quite reasonable because of the more rigid network of the glass structure in glass no. 2, due to the more amount of borate in the composition, which is expected to hinder the motion of the mobile sodium ions to some extent.

(ii) The very fact that Bismuth is responsible for electronic conduction in bismuth containing glasses was again substantiated by measuring conductivity with temperature on an another

non-bismuth glass (i.e. glass no. 4) by replacing bismuth oxide, by calcia, in glass no. 3. The result of the conductivity experiment on this glass is shown in Table 6. Here also the equation (4.1) was used and the nature of $\log (\ell/T)$ vs. $1/T$ plot, as shown in Figure 5, is a straight line all through the temperature range studied in this case. There is no change of slope observed even in the low temperature side which has been observed before with glass no. 2 also, strengthening our views that bismuth oxide is definitely responsible for electronic conduction in the bismuth containing glasses investigated.

The activation energy from the slope of the curve was calculated to be 26.4 kcal/mole, which is again consistent with the data of ordinary soda-lime-silica glasses as reported before.

The activation energy in glass no. 4 is also slightly higher than in glass no. 3 which seems to be quite reasonable because of the presence of more amount of calcia in this glass-structure, since bigger calcium ions are assumed to block the motion of moving sodium ions in the glass structure. Again, it can be said from the analysis of the data that the conductivity is higher in glass no. 4 than that in glass no. 2 due to the higher concentration of sodium ions in the former.

4.1.3 Conductivity Model in Amorphous Semiconductors:

We know that in all amorphous semiconductors the conductivity is expressed as follows:

$$\sigma = \sigma_0 \exp (-E/kT) \quad (4.2)$$

$$\text{or} \quad \rho = \rho_0 \exp (E/kT) \quad (4.3)$$

Here it is assumed that conduction is due to electrons (i.e. charge carriers) 'hopping' (tunnelling) between localised states near the Fermi energy. This is the process analogous to impurity conduction in heavily doped semiconductors.

Therefore, the data of glass nos. 1 and 3 (Bismuth containing glasses only) were plotted according to this model. The plots of $\log \rho$ vs. $1/T$ are shown in Figure 6 for both the glasses. In this case also there is a change of slope observed in both the glasses. The breaking points, at which the slopes of the $\log \rho$ vs. $1/T$ change, are approximately at the same temperatures, namely, 232°C for glass no. 1 and 184°C for glass no. 3, as observed before from the $\log (\rho/T)$ vs. $1/T$ plots for these two glasses, again confirming the fact that there is an influence of both electronic and ionic conduction in the overall conductivity of these glasses, i.e. there is a transition from a state of electronic conduction to a state of ionic conduction after certain temperatures, characteristic of these glasses.

4.1.3 Conductivity Model in Amorphous Semiconductors:

We know that in all amorphous semiconductors the conductivity is expressed as follows:

$$\sigma = \sigma_0 \exp (-E/kT) \quad (4.2)$$

$$\text{or } \rho = \rho_0 \exp (E/kT) \quad (4.3)$$

Here it is assumed that conduction is due to electrons (i.e. charge carriers) 'hopping' (tunnelling) between localised states near the Fermi energy. This is the process analogous to impurity conduction in heavily doped semiconductors.

Therefore, the data of glass nos. 1 and 3 (Bismuth containing glasses only) were plotted according to this model. The plots of $\log \rho$ vs. $1/T$ are shown in Figure 6 for both the glasses. In this case also there is a change of slope observed in both the glasses. The breaking points, at which the slopes of the $\log \rho$ vs. $1/T$ change, are approximately at the same temperatures, namely, 232°C for glass no. 1 and 184°C for glass no. 3, as observed before from the $\log (\rho/T)$ vs. $1/T$ plots for these two glasses, again confirming the fact that there is an influence of both electronic and ionic conduction in the overall conductivity of these glasses, i.e. there is a transition from a state of electronic conduction to a state of ionic conduction after certain temperatures, characteristic of these glasses.

However, it should be noted that this transition in the conduction behaviour of both these glasses does not take place exactly at a particular temperature which has been found out from the point of intersection of two straight lines in the respective plots. But this actually takes place over a range of temperature as can be seen from the curved portions of these two plots (Figures 4 and 5). The curved portions of the plots are ascribed to mixed effect of both ionic and electronic conduction, where no single phenomena, ionic or electronic, is predominantly operative.

It has been emphasized by Mott⁴⁵ that a straight line in a plot of $\ln \sigma$ against $1/T$ is expected only if hopping is between nearest neighbours. At the lower temperature side, it may become favourable for the electrons to tunnel to more distant sites, activation energy will fall, and ultimately the conductivity is expected to behave like

$$\ln \sigma = A - B/T^{1/4} \quad (4.4)$$

$$\text{or } \ln \sigma = -A + B/T^{1/4} \quad (4.5)$$

where A = A pre-exponential constant;

$$B = 1.7 \left(\frac{\alpha^3}{N(E_F) \cdot K} \right)^{1/4}$$

α = Decay constant for the localised state wave function;

$N(E_F)$ = Density of states in the Fermi level.

Since it was not known initially whether the hopping takes place between two nearest neighbours, a plot of $\log \epsilon$ against $1/T^{1/4}$ was also drawn to see the nature of the curve, which were straight lines for both glass nos. 1 and 3. Here also there is a change of slope in the curves showing some ionic contribution after certain temperatures for both the glasses, as shown in Figure 7. Since the nature of plot is straight line in the low temperature side, it can be concluded tentatively that the hopping of carriers is also taking place between the 'distant' sites. But the lack of conductivity data below room temperature makes it difficult to make a definite conclusion. However, it can be mentioned here that Clark's⁷⁰ data, on some other amorphous semiconductors fit quite well to a straight line even in the higher temperature region, the region in which our glasses were also studied.

4.2 Electrical Conductivity at Different Frequencies at Room Temperature:

Whether the electronic conduction is by hopping of electrons between two localised state can be quantified by the analysis of resistivity data with frequency. According to Mott⁴⁵ there is a frequency dependence of conductivity at lower temperature region which can be described by the following equation:

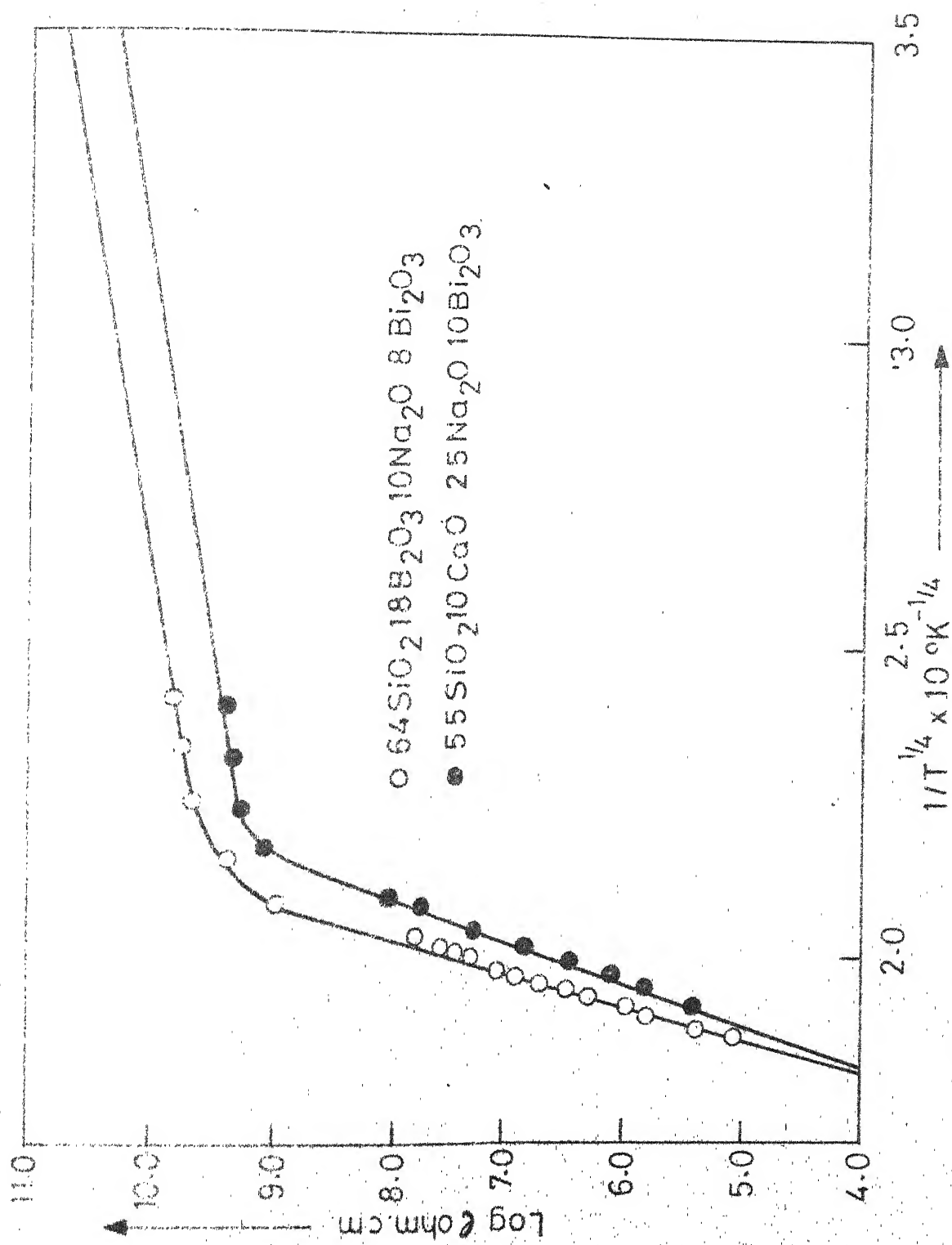


FIG.7. LOG ρ VS. $1/T^{1/4}$ PLOTS AT 1.0Kc/s.

$$\sigma = C \times f^n \quad (4.6)$$

where C = constant

f = frequency in cycles

If the value of the exponent n is approximately 0.8, then the conductivity is explained as arising due to hopping of electrons.

The equation (4.6) can be written as,

$$\sigma = C_1 \cdot f^{-n} \quad (4.7)$$

$$\text{or } \ln \sigma = C_1 + (-n) \ln f \quad (4.8)$$

where C_1 = a constant.

Therefore the data of resistivity against frequency were analysed according to the equation (4.8). The results are tabulated in Tables 7 to 10. $\log \sigma$ was plotted against $\log f$ for both glass nos. 1 and 3, as shown in Figure 8. The shape of the curves changes abruptly after certain frequency values showing a marked dependence of conductivity on frequency at this temperature (i.e. room temperature). The slopes of the $\log \sigma$ vs. $\log f$ plots yielded the values of 'n' to be 0.90 and 0.92, which are quite close to the theoretical value of 0.8, for glass nos. 1 and 3 respectively. Therefore it can be said that the conduction is due to hopping of electrons between two localised states in these glasses.

The hopping distance r_ω , may be defined⁷¹ in terms of a , the effective radius of the localised states wave functions and ν_0 , a phonon frequency characteristic of the material,

$$r_\omega = a \log (\nu_0/\omega) \quad (4.9)$$

Various densities are defined; N_S represent the total density of localised states; N_q the concentration of charged states; $N(E_f)$ the Fermi level density of states and N_c the concentration of carriers. Corresponding to N_q , one has a correlation length,

$$r_q = \left(\frac{4\pi}{3} N_q \right)^{-1/3} \quad (4.10)$$

and corresponding to N_S a mean separation between centres

$$r_S = \left[(4\pi/3) N_S \right]^{1/3} \quad (4.11)$$

By assuming that only one electron transitions contribute to the conductivity, Pollak⁷² goes on to prove that for the strongly correlated situation in which $r_\omega < r_q$,

$$\sigma(\omega) = \frac{\pi^2}{4} a \omega r_S^{-1} r_\omega^3 k N_c \quad (4.12)$$

and for the uncorrelated case in which $r_\omega > r_q$,

$$\sigma(\omega) = \pi^3/96 N^2(E_f) K T a \omega r_\omega^4 e^2 \quad (4.13)$$

It is instructive to calculate typical values of r_ω and r_q from the data shown in Figure 8 and extract information from the appropriate equation.

With the assumption that $a = 3 \text{ \AA}$ and taking $\nu_0 = 10^{12} \text{ Sec}^{-1}$, for a frequency $\omega = 10^4 \text{ c/s}$ we find from equation (4.9) that $r_\omega = 55 \text{ \AA}$.

From equation (4.12) using our experimentally determined values of k (6.8) and $\sigma (2.3 \times 10^{-10} \text{ ohm}^{-1} \text{ cm}^{-1})$, we obtain $N_c/r_S = 1.50 \times 10^{23} \text{ cm}^{-4}$.

Taking a total density of localized states $N_S = 10^{20} \text{ cm}^{-3}$, gives a mean separation distance $r_S = 13 \text{ \AA}$ and thus a concentration of carriers $N_c = 1.95 \times 10^{16} \text{ cm}^{-3}$. By further assuming that $N_q = 2 N_c$, we obtain $r_q = 122 \text{ \AA}$. This is for glass no. -1. For the reasonable figures quoted above we have $r_q > r_\omega$ thus justifying the use of equation (4.12) in our analysis. An attempt to fit our data to equation (4.13) resulted in an unphysically large value of $N(E_f)$. This then explains the insensitivity to temperature of the a.c. conductivity of the glass no. 1. The same thing has been found with the glass no. 3, where $r_\omega = 55 \text{ \AA}$ and $r_q = 128 \text{ \AA}$ showing that $r_q > r_\omega$. It can be concluded that even at temperatures above 300°K it appears that hopping conduction can occur within a very narrow band of localised states.

4.3 Conformance to some Recent Models:

(i) It has been shown by Schnakenberg⁷³ that for the case of disordered solids the conductivity can be split into two main contributions:

$$\sigma = \sigma(\text{opt}) + \sigma(\text{ac}), \quad (4.14)$$

$\sigma(\text{opt})$ and $\sigma(\text{ac})$ being the contribution activated purely by optical and purely by acoustic phonons respectively. $\sigma(\text{opt})$ is expected to dominate at higher temperatures and $\sigma(\text{ac})$ at lower temperatures. At intermediate temperatures both should be considered. It has been found⁷⁴ that

$$\sigma(\text{ac}) T^{1/2} \propto \exp(-B/T^{1/4}) \quad (4.15)$$

$$\text{and } \sigma(\text{opt}) T^{1/2} \propto \exp(-C/kT) \quad (4.16)$$

where B is as defined in equation (4.5);

and $C = \text{A constant} = (\Delta + 2W_p)^2 / 8W_p$

$\Delta = \text{Average energy separating one state from another.}$

$W_p = \text{Binding energy.}$

The present data for both the bismuth containing glasses (Tables 11 and 12) were analysed according to the equations (4.15) and (4.16). The plots of $\ln \sigma T^{1/2}$ vs. $1/T$ and $\ln \sigma T^{1/2}$ vs. $1/T^{1/4}$ are shown in Figures 9 and 10 for both the glasses. At the temperatures of investigation the plots of $\ln \sigma T^{1/2}$ vs. $1/T$ show more prominent straight lines than the $\ln \sigma T^{1/2}$ vs. $1/T^{1/4}$ plots because of the lack of data in the low temperature region (i.e. below room temperature).

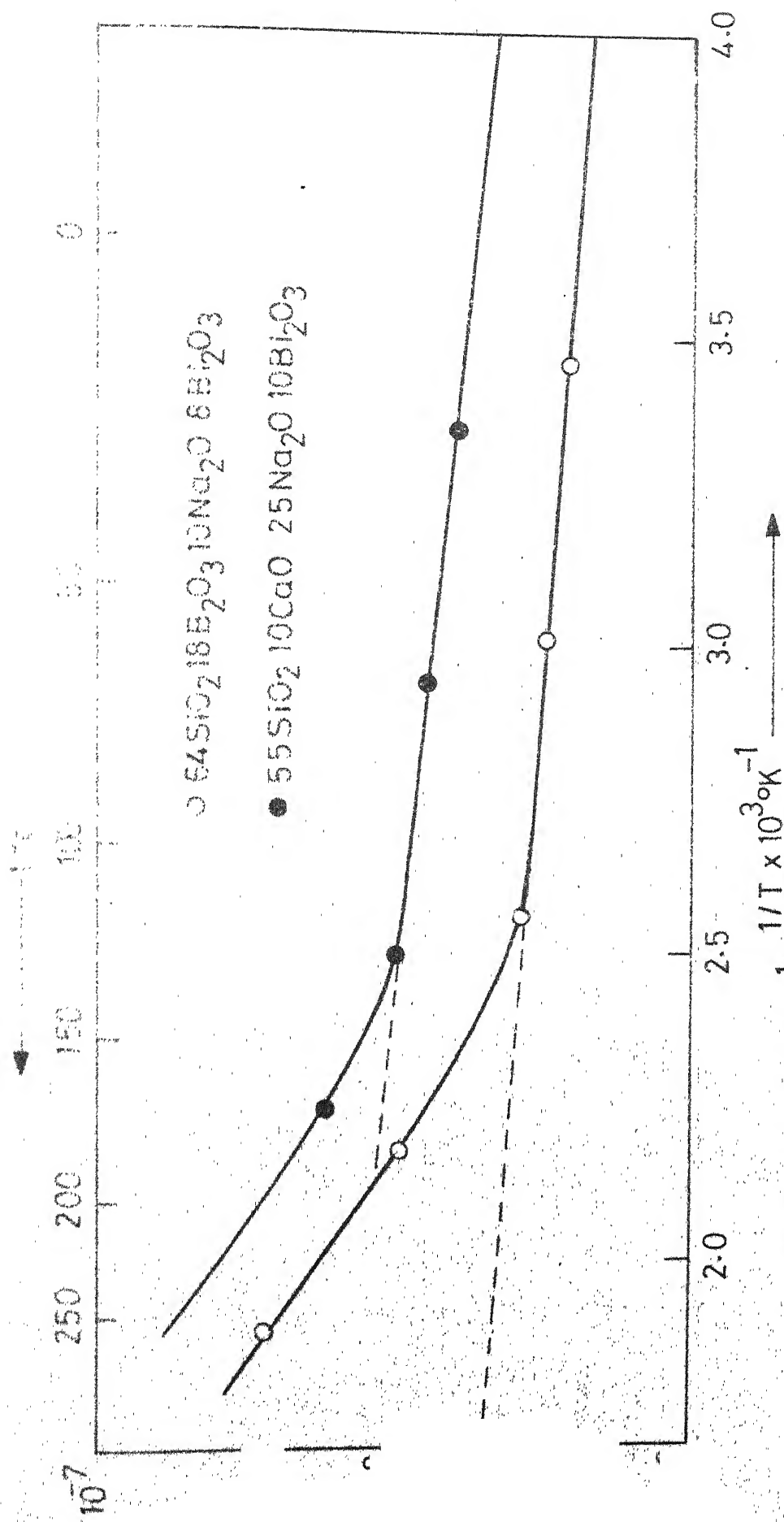


FIG. 9. $\log \sigma T^{1/2}$ VS $1/T$ PLOTS.

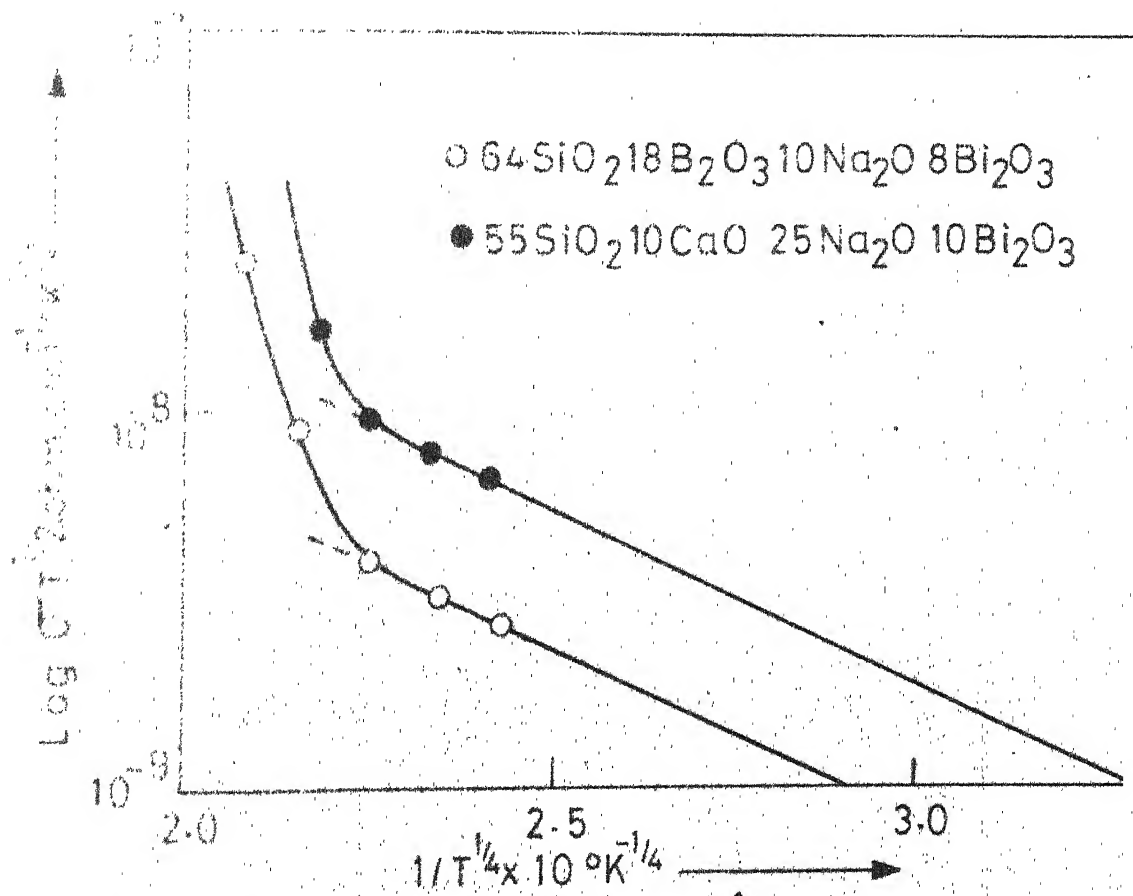


FIG. 10. $\text{LOG } \sigma T^{1/2}$ VS. $1/T^{1/4}$ PLOTS.

Therefore, at this stage, it can be only said that nearest neighbour optical phonon hopping is operative at the temperatures of this study, where it is expected that $\sigma(ac) \ll \sigma(opt)$, which seems to be consistent with the results of Greaves⁷⁴ on amorphous semiconductors based on $V_2O_5 - P_2O_5$.

(ii) It has been found by Schmid⁷⁵ by plotting $\log \rho$ vs. $1/T$ at different frequencies that conductivity is temperature independent at lower temperature region and is proportional to frequency. This effect has been associated with random glass lattice and small polaron as charge carriers.

The data for glass no. 1 (Tables 13 to 17) was analysed according to this model. The plot of $\log \rho$ vs. $1/T$ is shown in figure 11 which also shows the same type of behaviour as shown by the glasses of Schmid⁷⁵.

This according to Schmid⁷⁵ is due to the strongly localised electrons, which favours the formation of small polarons and these small polarons is believed to be the charge carriers.

Therefore, in this glass, small polaron conduction is assumed to be operative. However, the lack of conductivity data in the higher frequency region does not allow us to make any conclusive statement at this stage.

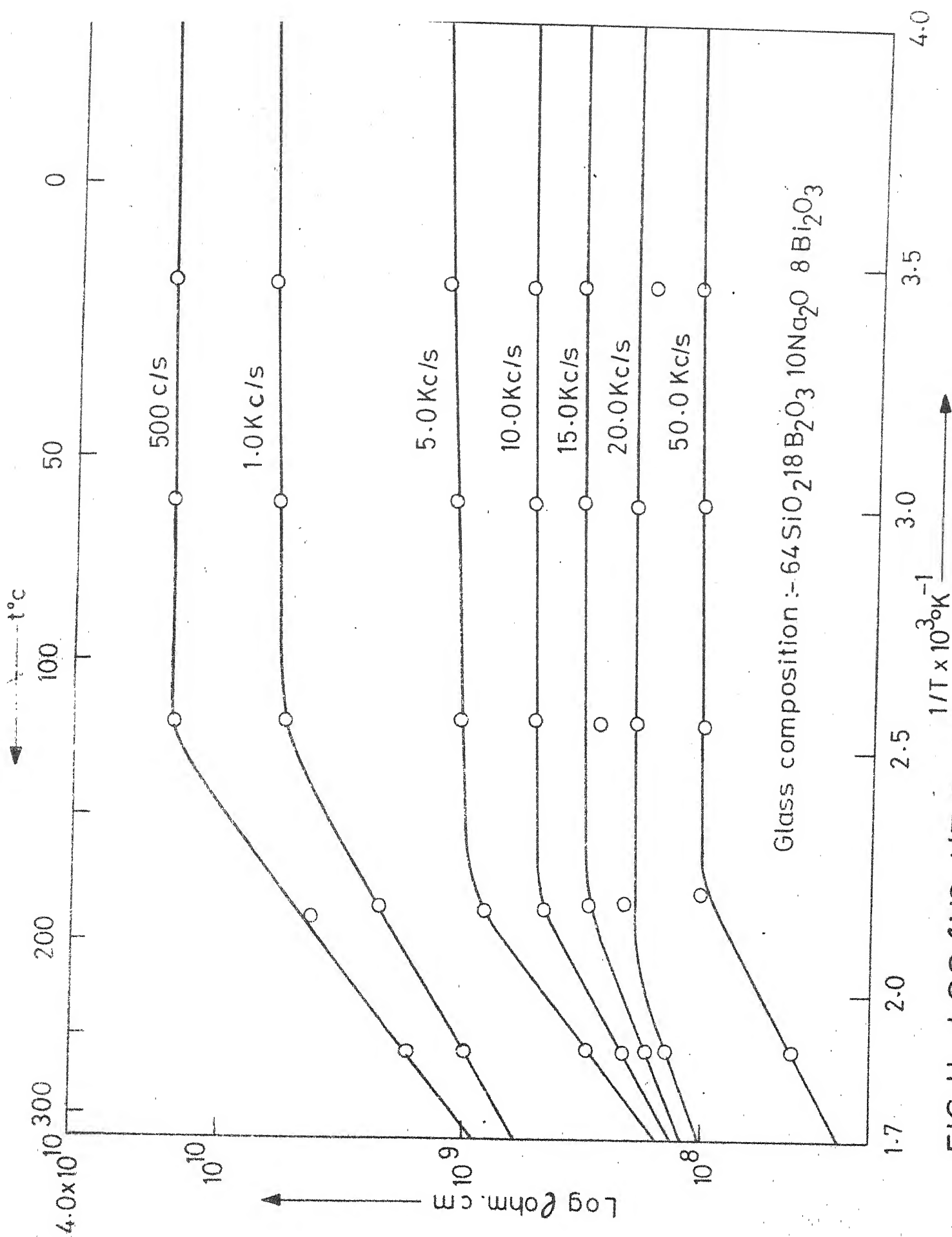


FIG. II. $\text{LOG } \rho$ VS. $1/T$ PLOTS AT DIFFERENT FREQUENCIES.

4.4 Dielectric Properties:

The results of the dielectric measurements are shown in Tables 13 to 17. The ϵ' vs. $\log f$ plots are shown in Figures 12a and 13 for all the temperatures. There is a good dispersion observed in the case of first three temperatures, namely 16°C , 59°C and 118°C . But at other two temperatures, namely 185°C and 260°C , the plots are somewhat different due to the influence of ionic contribution.

The ϵ'' vs. $\log f$ plots are shown in figures 12b and 14 for different temperatures. The first three curves for first three temperatures show some loss peaks at frequencies 15.0 kc/s, 20.0 kc/s and 27.0 kc/s respectively. Loss peaks are not prominent for other two temperatures again due to the ionic contribution. The dispersion of dielectric constant with frequency and occurrence of loss peaks in the ϵ'' vs. $\log f$ plots represent the presence of some 'relaxation' mechanism.

Whether, there is a distribution of relaxation mechanism present or not, Cole-Cole diagrams are drawn as shown in Figures 16 and 17. From these diagrams which show an arc of a circle for each temperature it is indicated that there is a distribution of relaxation time. Here also the Cole-Cole plots for the last two temperatures, namely 185°C and 260°C , are not very accurate showing the effect of ionic contribution. To understand the relaxation mechanism the following equation was used:

FIG. 12b. ϵ'' VS LOG f PLOTS.

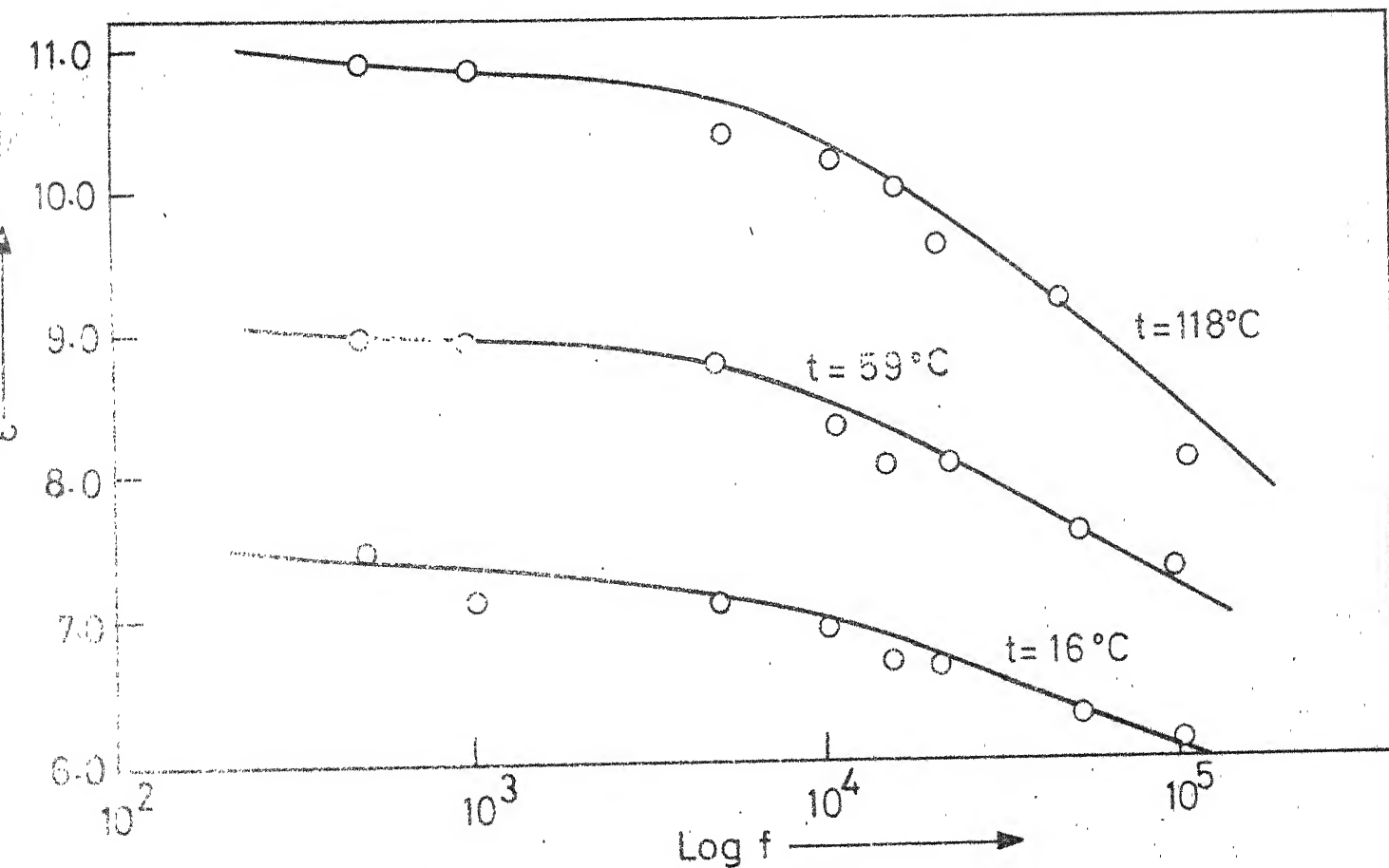
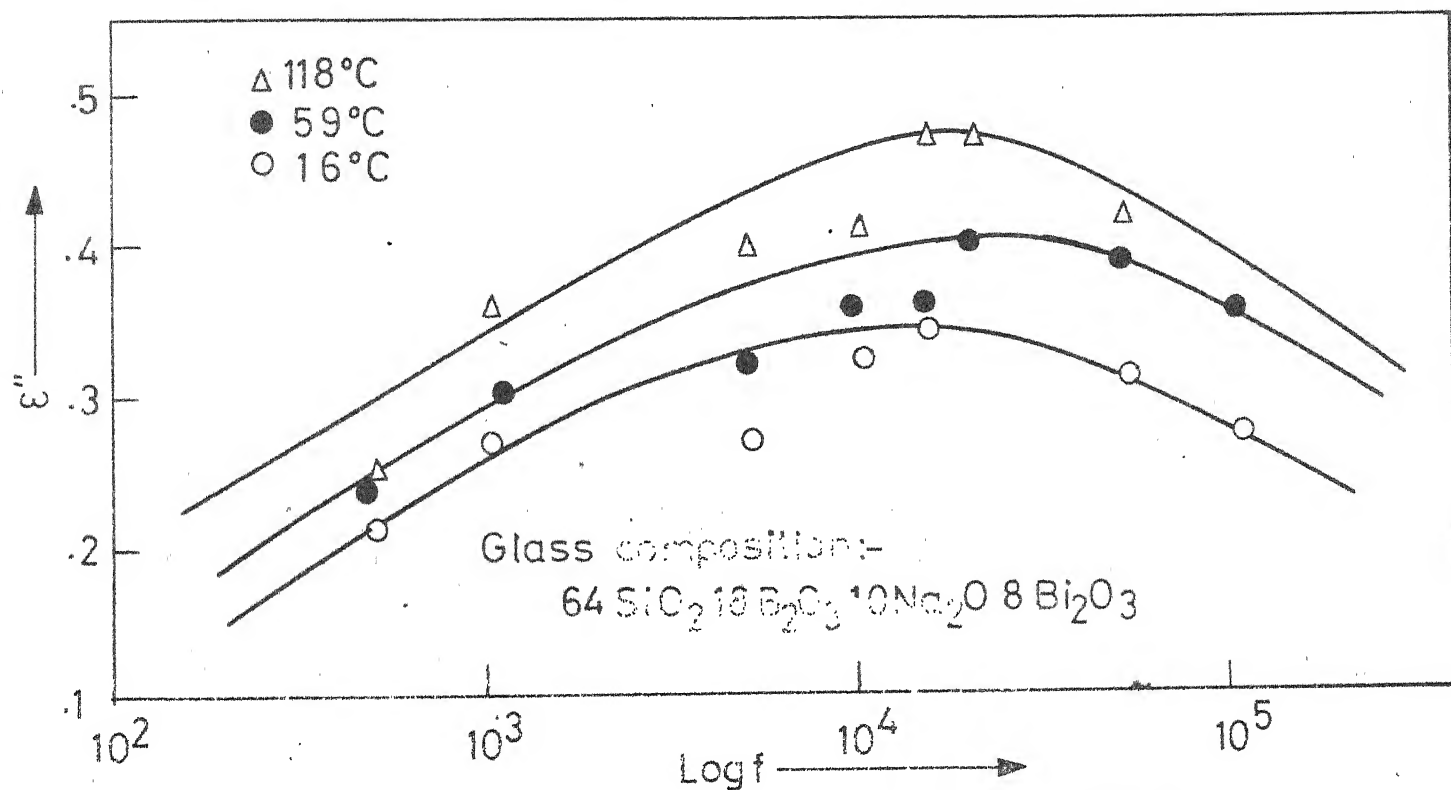


FIG. 12a. ϵ' VS LOG f PLOTS.

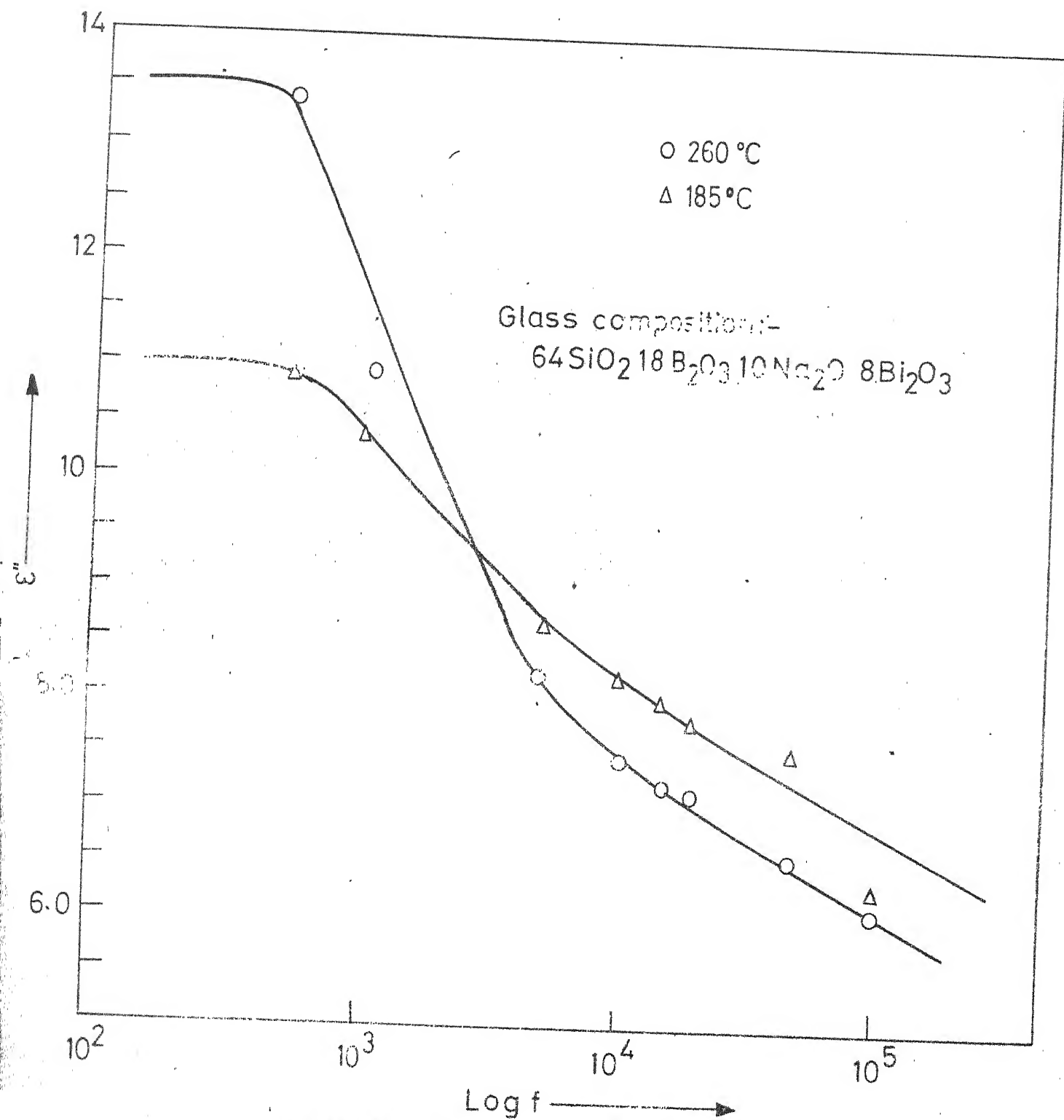


FIG.13 ε' VS LOG f PLOT.

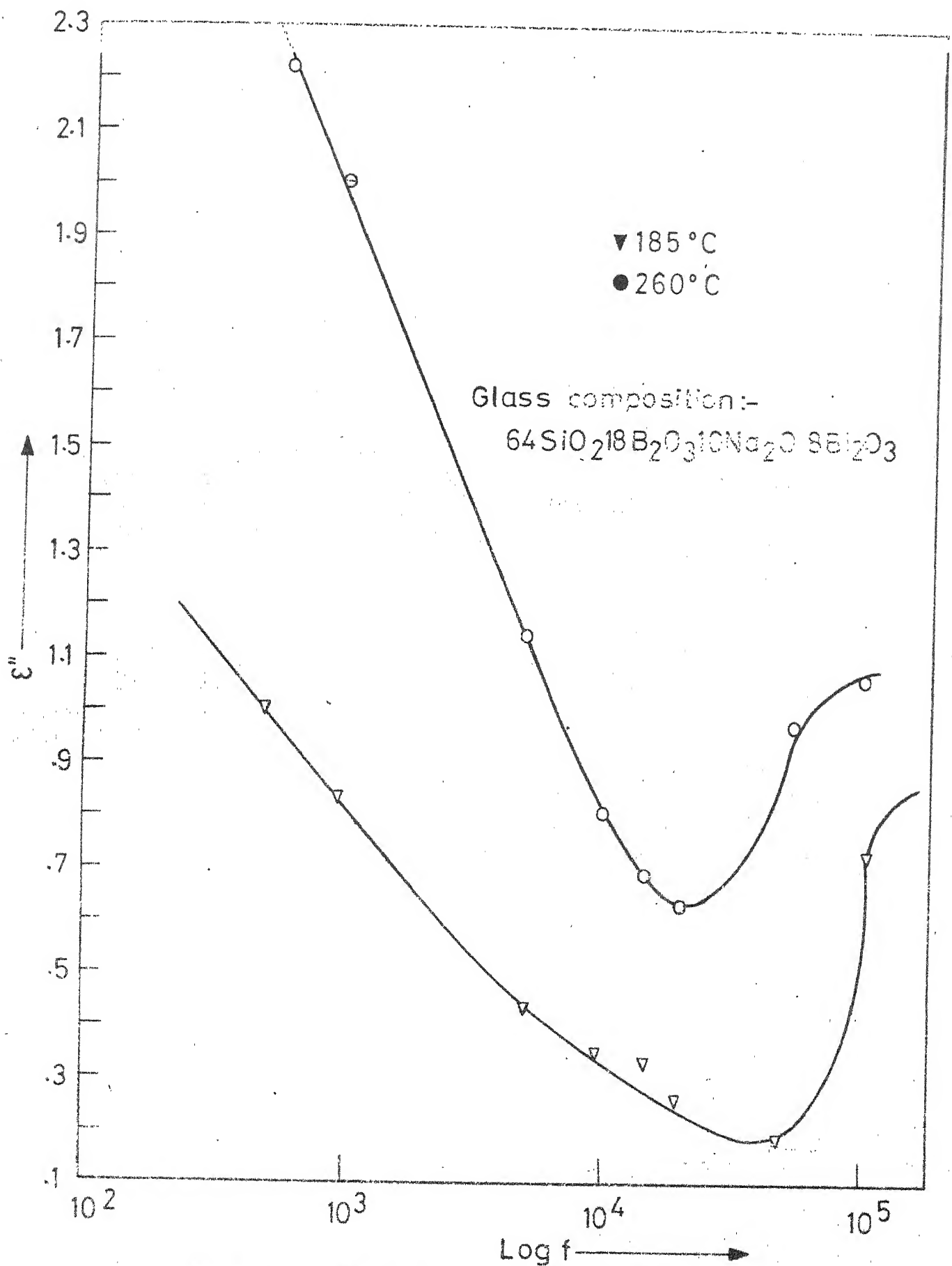


FIG. 14 ϵ'' VS LOG f PLOT.

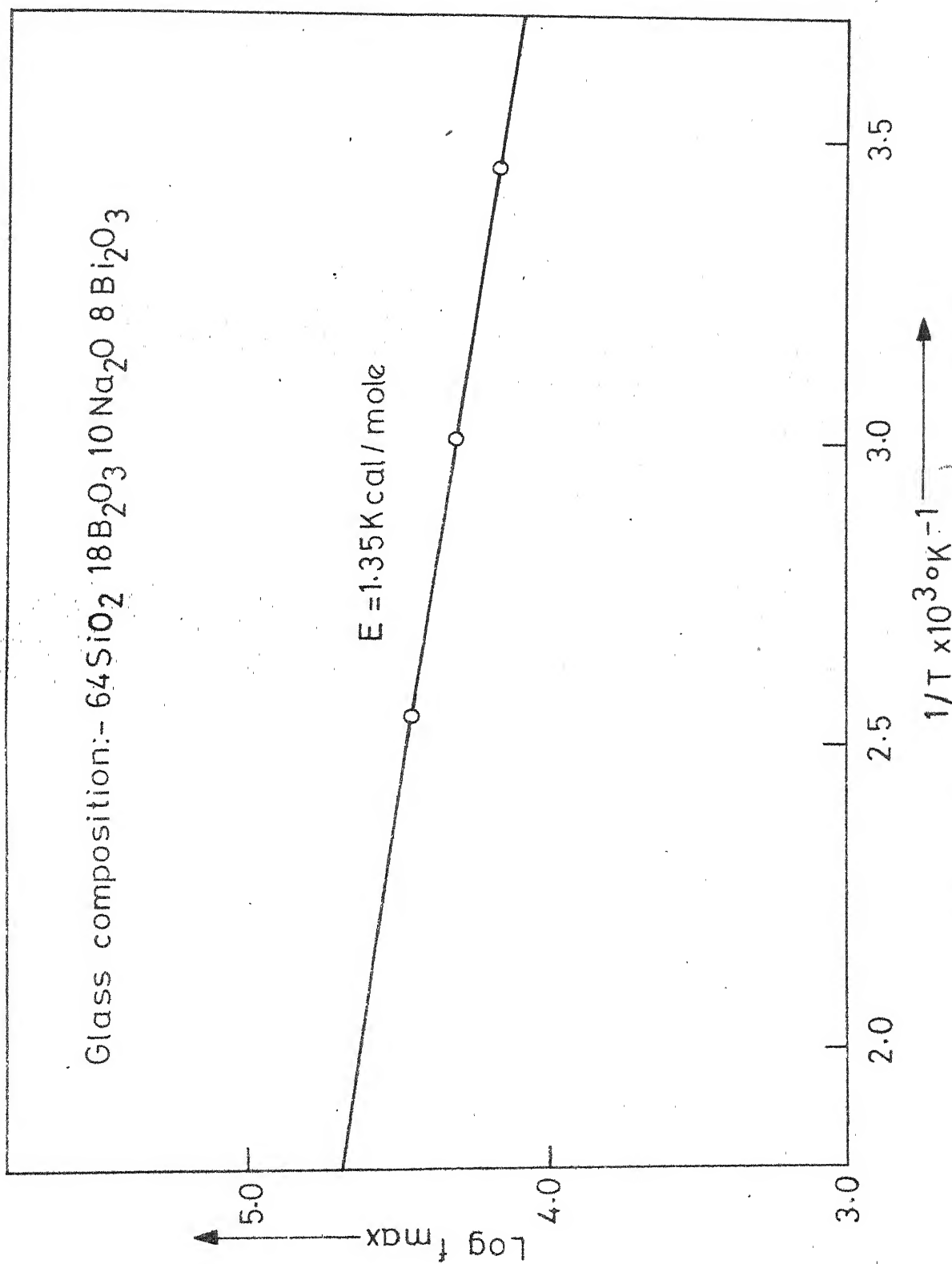


FIG. 15. $\text{LOG } f_{\max}$ VS $1/T$ PLOT.

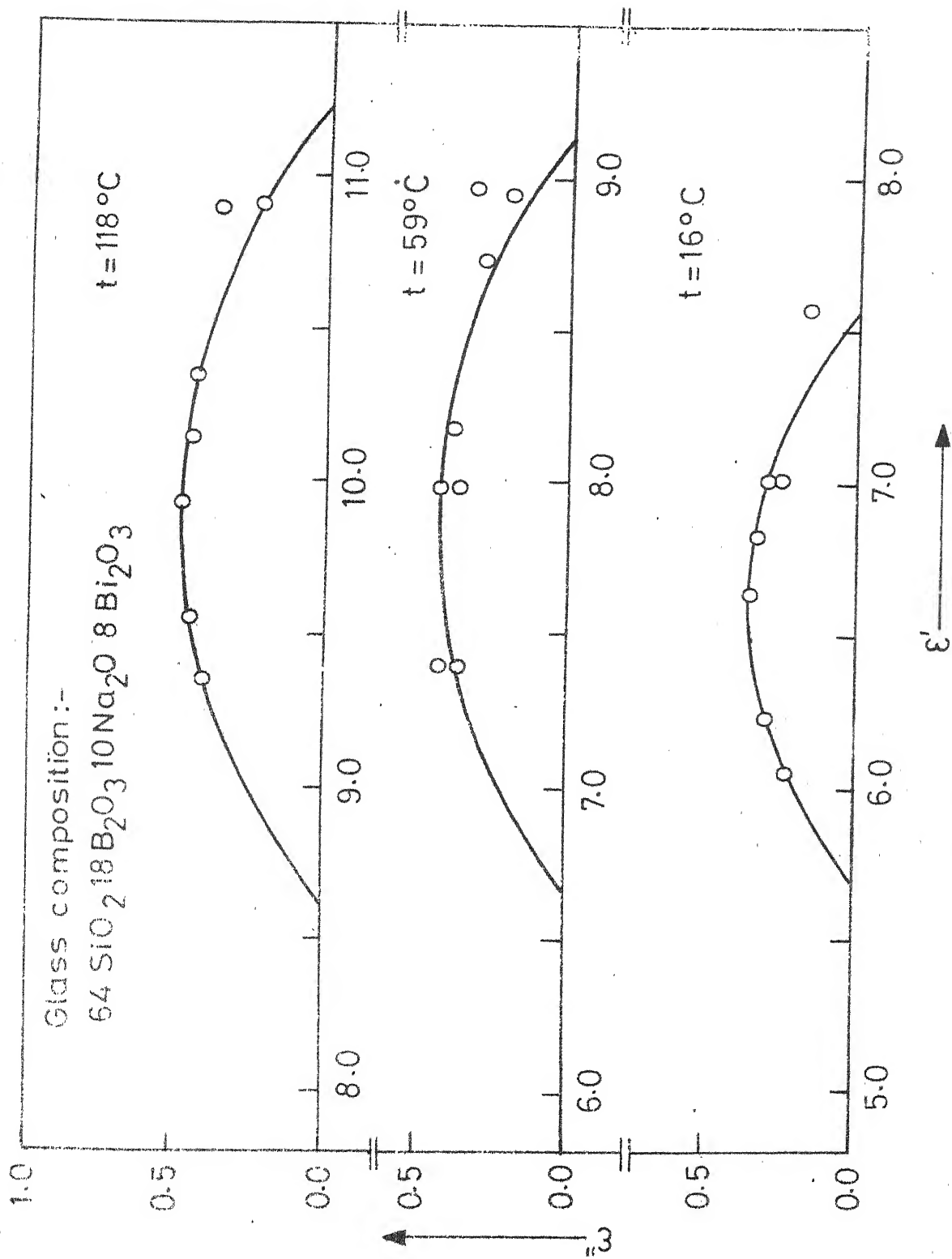


FIG. 16 COLE-COLE PLOTS.

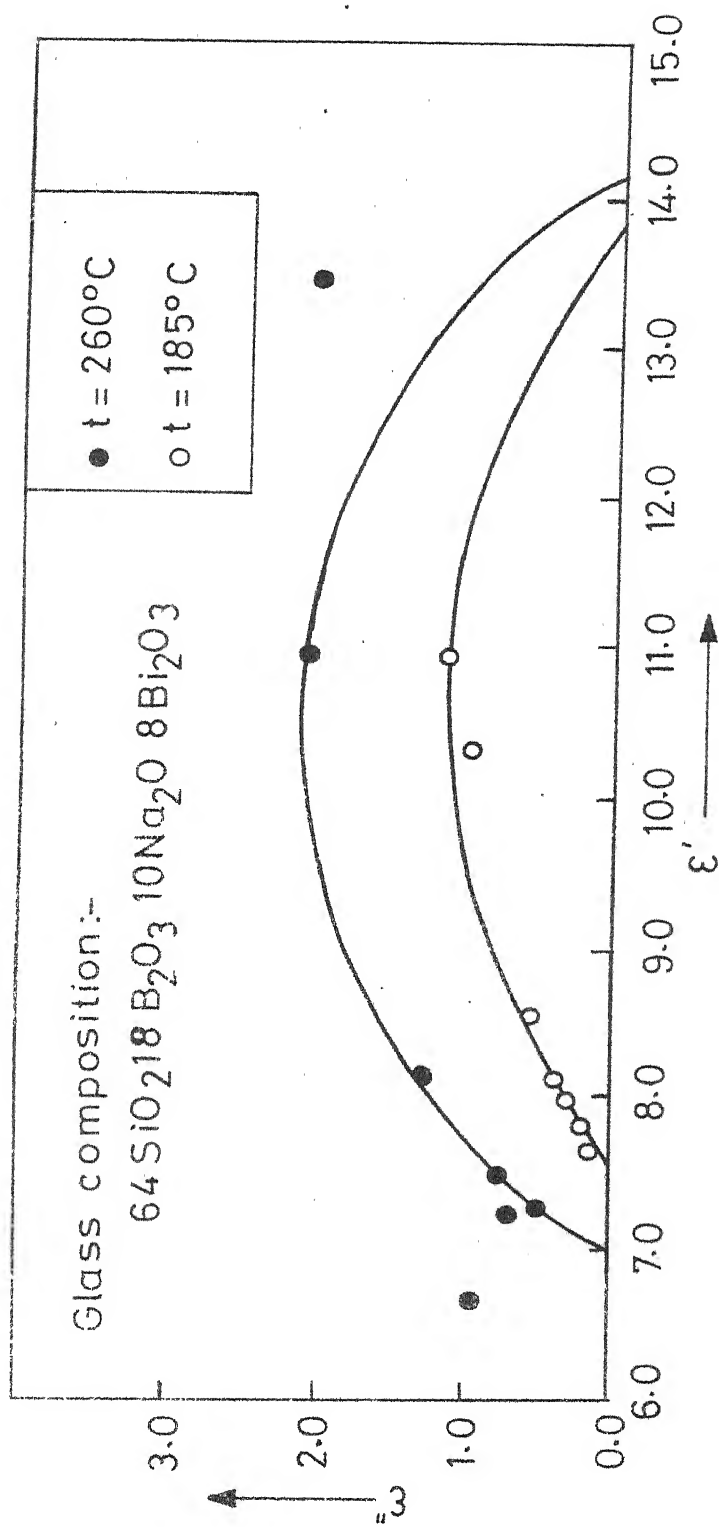


FIG.17. COLE-COLE PLOTS.

inhomogeneous conductor. The equation is

$$\tau \sim \epsilon_{\alpha} \epsilon_0 / \sigma(0) \quad (4.19)$$

where ϵ_0 is the permittivity of the free space and $\sigma(0)$ is the conductivity of the bulk glass in the limit $f \rightarrow 0$. The curve of ϵ'' against $x = \log [f/\sigma(0)]$ or $x = \log [f \times \ell(0)]$ shows a peak where $f = 1/2\pi\tau$, i.e. where $x = \log [1/2\pi \epsilon_{\infty}\epsilon_0]$.

Therefore the plots were drawn with ϵ'' against $\log [f \times \ell(0)]$ for three different temperatures, namely 16°C , 59°C and 118°C , as shown in Figure 18. All the loss peaks appear at the same value of x which is expected from this kind of Isard's plot. The peaks comes at approximately at the same place as that for ionically conducting glasses. According to Isard⁷⁶ this is due to the fact that the origin of dielectric relaxation must be the same in electronically conducting glasses as in ionically conducting glasses.

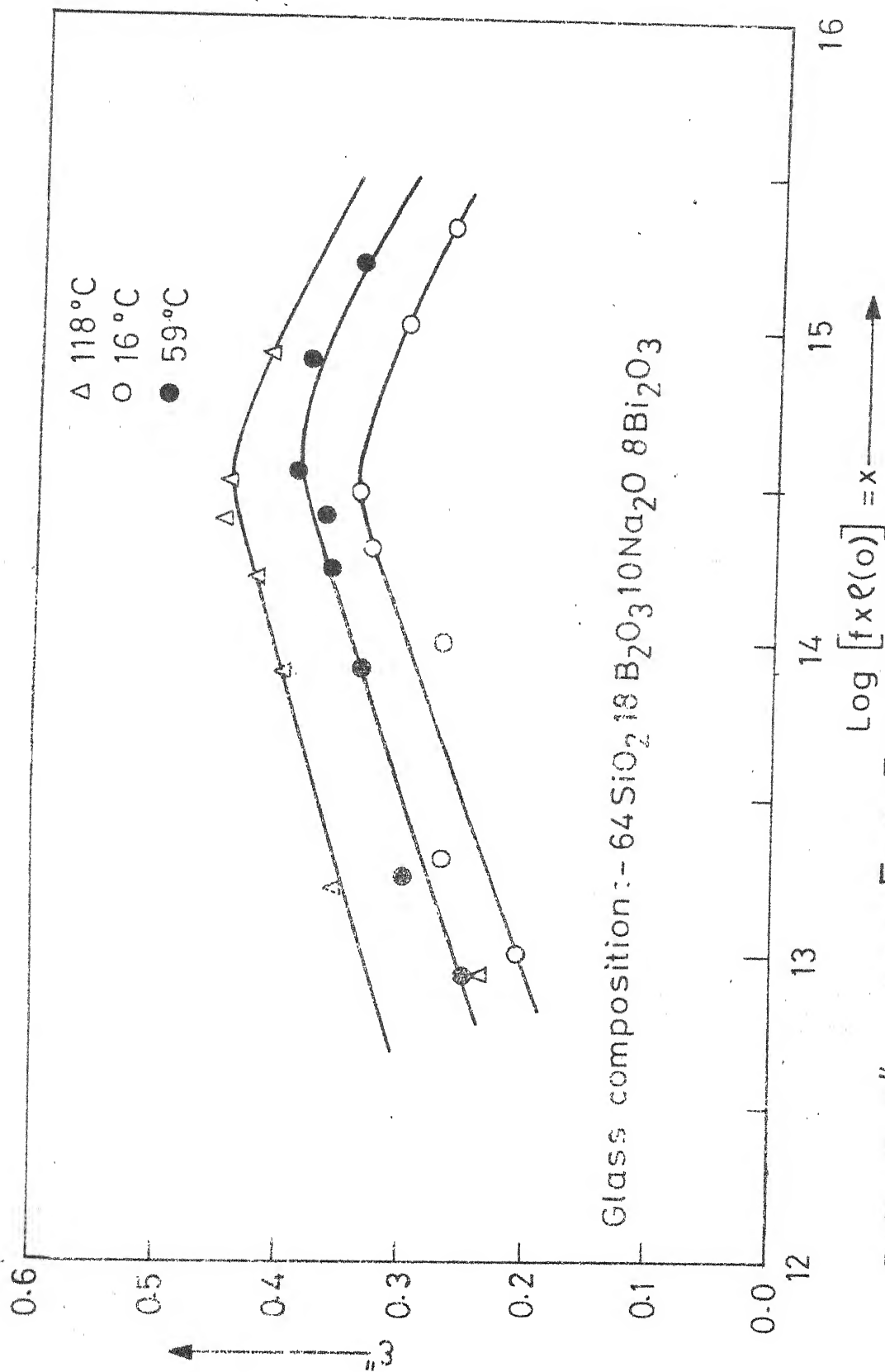


FIG. 18. ϵ'' VS $\text{LOG} [f \times e(o)]$ PLOT AT DIFFERENT TEMPERATURES.

V. CONCLUSIONS

1. There are two basic mechanisms of conduction ionic and electronic, contribute to the overall conductivity of the two bismuth-containing glasses studied in this work.
2. The ionic conduction is due to the field induced drift of Na^+ ions through the glass structure and the electronic conduction is due to the presence of Bismuth in these glasses.
3. The conductivity measurements of two non-bismuth glasses of the above two systems is quite conclusive of the effect of bismuth in the electronic conduction.
4. The electronic mechanism is ascribed to phonon-assisted hopping of electrons from one localised state to another.
5. The hopping of electrons is between nearest neighbours. The electron tunnelling between distant sites is less pronounced than between nearest sites.
6. Nearest neighbour optical phonon hopping is operative in the temperature of investigation for these glasses.
7. The formation of small polaron is quite favourable and it is believed that conduction is due to the transport of small polarons in the lower temperature region.

8. There is a distribution of relaxation time observed in one of these glasses.
9. There is a correspondence of the activation energy of the relaxation process with the activation energy of electronic conduction.

VI. APPENDIX

TABLE 1

Chemical Compositions of the Glasses.

Glass No.	Mole percent				
	SiO ₂	B ₂ O ₃	CaO	Na ₂ O	Bi ₂ O ₃
1.	64	18	—	10	8
2.	64	26	—	10	—
3.	55	—	10	25	10
4.	55	—	20	25	—

TABLE 2

Values of the Factors (A/l) for Different Glasses
and For Different Experiments.

Experiment	Glass No.	Area (A) (sq.cm.)	Thickness(l) (cm.)	(A/l) (c.m.)
Electrical conductivity at different tem- peratures at 1.0 kc/s	1.	1.886	0.325	5.803
	2.	1.886	0.350	5.389
	3.	1.886	0.192	9.824
	4.	1.886	0.3235	5.830
Electrical conductivity at Different fre- quencies at room temperature.	1.	5.307	0.365	20.13
	3.	4.53	0.225	14.54
Dielectric measurements	1.	0.0001886 Sq.meters	0.00325 meters	0.05802 meters

TABLE 3

Values of Resistivity at Different Temperatures for
Glass No. 1 at 1.0 Kc/s.

$t^{\circ}\text{C}$	$T^{\circ}\text{K}$	$1/T \times 10^{-3}$ $^{\circ}\text{K}^{-1}$	$1/T^{1/4}$ $\times 10^{-1}$ $^{\circ}\text{K}^{-1/4}$	R Ohms.	ρ Ohms.cm.	ρ/T ohm.cm. $^{\circ}\text{K}^{-1}$
16	289	3.460	2.425	1.095×10^9	6.354×10^9	2.199×10^7
59	332	3.012	2.343	9.995×10^8	5.799×10^9	1.747×10^7
118	391	2.554	2.249	8.333×10^8	4.835×10^9	1.235×10^7
185	458	2.183	2.162	3.733×10^8	2.166×10^9	4.730×10^6
260	533	1.876	2.081	1.540×10^8	8.935×10^8	1.676×10^6
308	581	1.724	2.037	1.1×10^7	6.383×10^7	1.101×10^5
325	598	1.672	2.022	7.0×10^6	4.061×10^7	6.792×10^4
341	614	1.629	2.009	5.0×10^6	2.901×10^7	4.725×10^4
555	628	1.592	1.997	3.5×10^6	2.031×10^7	3.233×10^4
375	648	1.543	1.982	1.8×10^6	1.044×10^7	1.612×10^4
389	662	1.510	1.972	1.3×10^6	7.543×10^6	1.140×10^4
404	677	1.477	1.961	8.3×10^5	4.818×10^6	7.114×10^3
421	694	1.441	1.948	4.8×10^5	2.785×10^6	4.013×10^3
435	708	1.413	1.938	3.5×10^5	2.031×10^6	2.869×10^3
455	728	1.374	1.925	1.6×10^5	9.283×10^5	1.276×10^3
491	764	1.309	1.902	1.2×10^5	6.963×10^5	9.114×10^2
512	785	1.274	1.889	4.0×10^4	2.321×10^5	2.956×10^2
519	792	1.263	1.885	2.0×10^4	1.161×10^5	1.465×10^2

TABLE 4

Values of Resistivity at Different Temperatures for
Glass No. 2 At 1.0 Kc/s.

$t^{\circ}\text{C}$	$T^{\circ}\text{K}$	$1/T \times 10^{-3}$ $^{\circ}\text{K}^{-1}$	R Ohm.	ρ Ohm.cm.	ρ/T Ohm.cm. $^{\circ}\text{K}^{-1}$
143	416	2.404	8.658×10^9	4.666×10^{10}	1.121×10^8
162	435	2.299	1.435×10^9	7.732×10^9	1.778×10^7
181	454	2.203	2.665×10^8	1.436×10^9	3.163×10^6
221.	494	2.023	1.1×10^7	5.928×10^7	1.200×10^5
253	526	1.901	1.38×10^6	7.437×10^6	1.414×10^4
277	550	1.818	3.23×10^5	1.741×10^6	3.164×10^3
314	587	1.704	4.35×10^4	2.344×10^5	3.994×10^2

TABLE 5

Values of Resistivity at Different Temperatures for
Glass No. 3 at 1.0 Kc/s.

$t^{\circ}\text{C}$	$T^{\circ}\text{K}$	$1/T \times 10^{-3}$ $^{\circ}\text{K}^{-1}$	$1/T \times 10^{-1}$ $^{\circ}\text{K}^{-1/4}$	R Ohms.	ρ Ohms. cm.	ρ/T Ohm. cm. $^{\circ}\text{K}^{-1}$
25	298	3.356	2.407	2.735×10^8	2.686×10^9	9.016×10^6
67	340	2.941	2.329	2.451×10^8	2.407×10^9	7.081×10^6
127	400	2.500	2.237	2.041×10^8	2.004×10^9	5.012×10^6
172	445	2.247	2.177	1.277×10^8	1.255×10^9	2.820×10^6
237	510	1.961	2.104	1.10×10^7	1.080×10^8	2.118×10^5
264	537	1.862	2.077	6.15×10^6	6.040×10^7	1.125×10^5
298	571	1.752	2.046	1.84×10^6	1.807×10^7	3.165×10^4
328	601	1.663	2.019	6.90×10^5	6.776×10^6	1.127×10^4
360	633	1.580	1.994	2.90×10^5	2.848×10^6	4.500×10^3
389	662	1.510	1.972	1.35×10^5	1.326×10^6	2.003×10^3
416	689	1.452	1.952	7.00×10^4	6.876×10^5	9.984×10^2
467	740	1.352	1.917	2.40×10^4	2.357×10^5	3.185×10^2

TABLE 6

Values of Resistivity at Different Temperatures for
Glass No. 4 at 1.0 Kc/s.

$t^{\circ}\text{C}$	$T^{\circ}\text{K}$	$1/T \times 10^{-3}$ $^{\circ}\text{K}^{-1}$	R Ohms.	ϵ Ohm.cm.	ϵ/T Ohm.cm. $^{\circ}\text{K}^{-1}$
104	377	2.653	5.896×10^9	3.438×10^{10}	9.118×10^7
119	392	2.551	1.540×10^9	8.978×10^9	2.291×10^7
143	416	2.404	2.309×10^8	1.346×10^9	3.236×10^6
168	441	2.268	4.352×10^7	2.537×10^8	5.754×10^5
202	475	2.015	4.65×10^6	2.711×10^7	5.464×10^4
240	513	1.949	7.15×10^5	4.196×10^6	8.125×10^3
270	543	1.842	1.70×10^5	9.910×10^5	1.826×10^3
315	588	1.700	3.25×10^4	1.895×10^5	3.222×10^2
344	617	1.621	1.08×10^4	6.296×10^4	1.021×10^2

TABLE 7

Values of Resistivity at Different Frequencies for
Glass No. 1 at Room Temperature (From Capacitance
Bridge Experiment).

f Kc/s	C_x	D_x	R (Ohm.)	ϵ (Ohm.-cm)
1	11.50	0.03040	4.555×10^8	6.624×10^9
2	11.32	0.01737	4.050×10^8	5.889×10^9
5	11.40	0.009766	2.861×10^8	4.161×10^9
10	11.40	0.008179	1.708×10^8	2.483×10^9
20	11.42	0.01134	6.148×10^7	8.941×10^8
50	11.40	0.004546	6.145×10^7	8.937×10^8
60	11.35	0.004110	5.690×10^7	8.273×10^8
100	11.32	0.005136	2.738×10^7	3.982×10^8

TABLE 8

Values of Resistivity at Different Frequencies for
Glass No. 1 At Room Temperature (From Boonton
Q-Meter Experiment)

f	C_1	C_2	Q_1	Q_2	R Ohm.	ϵ Ohm.cm.
100 Kc/s	89	80	123	112	2.241×10^7	3.258×10^8
500 "	302	290	186	180	5.884×10^6	8.557×10^7
1 Mc/s	91	82	224	198	2.985×10^6	4.345×10^7
3 "	103	94	206	186	9.872×10^5	1.435×10^7
5 "	442	428	198	194	6.918×10^5	1.006×10^7
10 "	93	84	224	203	3.707×10^5	5.388×10^6
20 "	116	107	246	224	1.718×10^5	2.498×10^6
25 "	71	63	253	217	1.368×10^5	1.989×10^6
40 "	55	42	260	220	1.094×10^5	1.592×10^6

TABLE 9

Values of Resistivity at Different Frequencies for
Glass No. 3 at Room Temperature (From Capacitance
Bridge Experiment)

f (Kc/s)	C_x	D_x	R Ohm.	ρ Ohm.cm.
1.0	33.9	0.07506	6.258×10^7	1.260×10^9
1.5	29.6	0.05811	6.170×10^7	1.242×10^9
2.0	29.6	0.04554	5.906×10^7	1.189×10^9
10.0	30.9	0.01416	3.639×10^7	7.324×10^8
15.0	28.8	0.01233	2.990×10^7	6.019×10^8
20.0	28.7	0.008246	3.364×10^7	6.770×10^8
50.0	28.7	0.005610	1.977×10^7	3.980×10^8
100.0	28.6	0.005019	1.109×10^7	2.231×10^8

TABLE 10

Values of Resistivity at Different Frequencies for
Glass No. 3 at Room Temperature (From Boonton
Q-meter Experiment)

f	C_1	C_2	Q_1	Q_2	R Ohm.	ρ Ohm.cm.
100.0 Kc/s	89	69	124	105	1.226×10^7	2.468×10^8
500.0 Kc/s	390	371	183	175	3.268×10^6	6.579×10^7
1.0 Mc/s	90	70	225	183	1.735×10^6	3.491×10^7
1.5 Mc/s	436	417	167	160	9.292×10^5	1.870×10^7
3.0 Mc/s	102	82	220	179	4.998×10^5	1.006×10^7
5.0 Mc/s	391	372	176	169	3.469×10^5	6.982×10^6
10.0 Mc/s	92	72	229	197	2.440×10^5	4.911×10^6
20.0 Mc/s	115	95	253	218	1.091×10^5	2.196×10^6
28.0 Mc/s	64	35	259	180	6.241×10^4	1.256×10^6

TABLE 11

Values of Conductivity at Different Temperatures for
Glass No. 1.

$T^{\circ}\text{K}$	$1/T \times 10^{-3}$ $^{\circ}\text{K}^{-1}$	$1/T^{1/4} \times 10^{-1}$ $^{\circ}\text{K}^{-1/4}$	$T^{1/2}$ $^{\circ}\text{K}^{1/2}$	ρ ohm.cm.	σ $(\text{ohm.cm.})^{-1}$	$\sigma T^{1/2}$ $(\text{ohm.cm.})^{-1}^{\circ}\text{K}^{1/2}$
289	3.460	2.425	17.00	6.354×10^9	1.573×10^{-10}	2.675×10^{-5}
332	3.012	2.343	18.22	5.799×10^9	1.724×10^{-10}	3.145×10^{-9}
391	2.554	2.249	19.77	4.835×10^9	2.068×10^{-10}	4.091×10^{-9}
458	2.183	2.162	21.40	2.166×10^9	4.618×10^{-10}	9.879×10^{-9}
533	1.876	2.081	23.09	8.935×10^8	1.119×10^{-9}	2.583×10^{-3}

TABLE 12

Values of Conductivity at Different Temperatures for
Glass No. 3

$T^{\circ}\text{K}$	$1/T \times 10^{-3}$ $^{\circ}\text{K}^{-1}$	$1/T^{1/4} \times 10^{-1}$ $^{\circ}\text{K}^{-1/4}$	$T^{1/2}$ $^{\circ}\text{K}^{1/2}$	ρ ohm.cm.	σ $(\text{ohm.cm.})^{-1}$	$\sigma T^{1/2}$ $(\text{ohm.cm.})^{-1}^{\circ}\text{K}^{1/2}$
298	3.356	2.407	17.26	2.686×10^9	3.723×10^{-10}	6.427×10^{-9}
340	2.941	2.329	18.44	2.407×10^9	4.156×10^{-10}	7.661×10^{-9}
400	2.500	2.237	20.00	2.004×10^9	4.991×10^{-10}	9.982×10^{-9}
445	2.247	2.177	21.10	1.255×10^9	7.969×10^{-10}	1.648×10^{-8}

TABLE 13

Dielectric and Resistivity Data at Different Frequencies
for Glass No. 1 at 16°C

f (Kc/s)	C_x	$\tan \delta =$ D_x	R_x (Ohm.)	ρ_x (Ohm.cm)	ϵ'	ϵ''
0.5	3.9	0.02610	3.128×10^9	1.815×10^{10}	7.591	0.1981
1.0	3.6	0.04039	1.095×10^9	6.354×10^9	7.006	0.2830
5.0	3.6	0.03656	2.419×10^8	1.404×10^9	7.006	0.2562
10.0	3.6	0.04605	9.879×10^7	5.732×10^8	6.813	0.3137
15.0	3.4	0.05182	6.024×10^7	3.495×10^8	6.618	0.3430
20.0	3.4	0.09510	2.462×10^7	1.429×10^8	6.618	0.6294
50.0	3.2	0.04848	2.053×10^7	1.191×10^8	6.227	0.3018
100.0	3.1	0.04302	1.193×10^7	6.921×10^7	6.034	0.2596

TABLE 14

Dielectric and Resistivity Data at Different Frequencies
For Glass No. 1 at 59°C.

f (kc/s)	C_x	$\tan \delta =$ D_x	R_x (Ohm.)	ρ_x (Ohm.cm)	ϵ'	ϵ''
0.5	4.6	0.02519	2.749×10^9	1.595×10^{10}	8.954	0.2255
1.0	4.6	0.03469	9.995×10^8	5.799×10^9	8.954	0.3106
5.0	4.5	0.03649	1.939×10^8	1.126×10^9	8.758	0.3196
10.0	4.2	0.04176	9.080×10^7	5.269×10^8	8.174	0.3413
15.0	4.1	0.04283	6.045×10^7	3.508×10^8	7.980	0.3418
20.0	4.1	0.05006	3.879×10^7	2.251×10^8	7.980	0.3995
50.0	3.8	0.05424	1.545×10^7	8.964×10^7	7.396	0.4012
100.00	3.8	0.04668	8.976×10^6	5.208×10^7	7.396	0.3452

TABLE 15

Dielectric And Resistivity Data at Different Frequencies
For Glass No. 1 at 118°C.

f (Kc/s)	C_x	$\tan \delta =$ D_x	R_x Ohm.	ρ_x Ohm.cm.	ϵ'	ϵ''
0.5	5.6	0.02097	2.711×10^9	1.573×10^{10}	10.90	0.2286
1.0	5.6	0.03412	8.333×10^8	4.835×10^9	10.90	0.3719
5.0	5.3	0.03758	1.599×10^8	9.279×10^8	10.31	0.3877
10.0	5.2	0.03979	7.695×10^7	4.465×10^8	10.12	0.4027
15.0	5.1	0.04788	4.346×10^7	2.522×10^8	9.926	0.4752
20.0	4.9	0.04839	3.359×10^7	1.949×10^8	9.537	0.4615
50.0	4.8	0.04336	1.530×10^7	8.878×10^7	9.342	0.4051
100.0	4.1	0.1087	3.572×10^6	2.072×10^7	7.980	0.8676

TABLE 16

Dielectric And Resistivity Data at Different Frequencies
For Glass No. 1 At 185°C.

f (Kc/s)	C_x	$\tan \delta =$ D_x	R_x (Ohm.)	ρ_x (Ohm.cm.)	ϵ'	ϵ''
0.5	5.6	0.09319	6.243×10^8	3.622×10^9	10.90	1.0160
1.0	5.3	0.08048	3.733×10^8	2.166×10^9	10.31	0.8303
5.0	4.4	0.05018	1.422×10^8	8.250×10^8	8.565	0.4297
10.0	4.2	0.04562	8.310×10^7	4.821×10^8	8.174	0.3729
15.0	4.1	0.04320	5.992×10^7	3.476×10^8	7.980	0.3447
20.0	4.0	0.03693	5.391×10^7	2.522×10^8	7.785	0.2876
50.0	3.9	0.02280	3.580×10^7	2.077×10^8	7.591	0.1731
100.0	3.2	0.1330	3.818×10^6	2.215×10^7	6.227	0.8283

TABLE 17

Dielectric and Resistivity Data at Different Frequencies
For Glass No. 1 At 260°C.

f (Kc/s)	C_x	$\tan \delta =$ D_x	R_x (Ohm.)	ϵ_x (Ohm.cm)	ϵ'	ϵ''
0.5	6.9	0.1644	2.807×10^8	1.629×10^9	13.43	2.2080
1.0	5.6	0.1846	1.540×10^8	8.935×10^8	10.90	2.0120
5.0	4.2	0.1396	5.429×10^7	3.150×10^8	8.174	1.1410
10.0	3.8	0.1081	3.873×10^7	2.247×10^8	7.396	0.7995
15.0	3.7	0.09541	3.007×10^7	1.745×10^8	7.201	0.6369
20.0	3.7	0.03758	2.457×10^7	1.426×10^8	7.201	0.6306
50.0	3.4	0.1478	6.336×10^6	3.676×10^7	6.618	0.9781
100.0	3.2	0.1667	2.984×10^6	1.732×10^7	6.227	1.038

REFERENCES

1. J.F. Dewald, A.D. Pearson, W.R. Northover and W.F. Peck J. Oral Presentations and 1000-word abstract, Electrochem. Soc. Meeting, Los Angeles, May, 1962. Also J. Electrochem. Soc. 109 (1962) 243C.
2. A.D. Pearson, J.F. Dewald, W.R. Northover and W.F. Peck J. in Advances in Glass Technology (Plenum Press, New York 1962) p. 357. Also in: Advances in Glass Technology Part 2 (Plenum Press, New York, 1963)p. 145.
3. B.T. Kolomiets and E.A. Lebedev, Radio Engg. Electron, USSR, 8(1963) 1941.
4. S.R. Ovshinsky, Phys. Rev. Letters, 21 (1968), 1450.
5. Y. Ashara and T. Izumitani, J. Non-Cryst. Solids, 11 (1973) 407.
6. J.R. Bosnell and C.B. Thomas, J. Phys. (D), 5 (1972) L29.
7. C. Fieldman and W.A. Gutierrez, J. Appl. Phys., 39 (1968), 2474.
8. J.R. Bosnell and J.A. Sawage, J. Mater. Sci., (1972).
9. P.O. Silva, G. Dir, C. Griffiths, J. Non-Crystalline Solids, 2 (1970) 316.
10. F. Drake, I.F. Scanlova and A. Engel, Phys. Stat. Solidi, 32 (1969) 193.
11. M.H. Omar, EL-Hamamsy and A.M. Bishay, Proceedings of IXth International Glass Congress, Paris, 1971.
12. D. Chakravorty, U.K. Patent Application No. 41515/71 (French Patent No. 72/31218).
13. D. Chakravorty, Appl. Phys. Letters, Vol. 24, No. 2, (1974) 62.
14. G. Bush et.al., Phys. Letters, A33 (1970) 64.
15. L.A. Coward, J. Non-Cryst. Solids, 6 (1971) 107.
16. J.R. Bosnel and C.B. Thomas, Solid State Electron., 15 (1972) 1261.

17. C.B. Thomas et.al., Electron Letters, 8 (1972) 447.
18. S.R. Ovshinsky and H.Fritzsche, IEEE Trans.,(1973).
19. C.B. Thomas et.al., Phil. Mag., 26 (1972) 617.
20. A.D. Pearson, J. Non-Cryst. Solids, 2 (1970) 1.
21. K.W. Boer, Phys. Stat. Solidi (a), 4(1971) 571.
22. T.Kaplan and D. Adler, Appl. Phys. Letters, 19(1971) 418.
23. H.K. Henisch and R.W. Pryor, Solid State Electronics, 14 (1971) 765.
24. B.G. Bagley and H.E. Bair, J. Non-Cryst. Solids, 2 (1970) 155.
25. A.D. Pearson and C.E. Miller, Appl. Phys. Letters, 14 (1970) 280.
26. J.R. Bosnell and C.B. Thomas, Phil. Mag., 27 (1973) 665.
27. K. Tanaka et.al., Solid State Commun., 8 (1970) 75.
28. A. Bienstock et.al., J. Non-Crystalline Solids, 2(1970) 347.
29. R. Uttecht et.al., J. Non-Cryst. Solids, 2(1970) 358.
30. R. Pinto, J. Non-Cryst. Solids, 6(1971) 187.
31. N.F. Mott, Phil. Mag., 24 (1971) 911.
32. W. Van Roas Broeck, Phys. Rev. Letters, 28 (1972) 1120.
33. S.R. Ovshinsky, Appl. Phys. Letters,
34. B.T. Kolomiets, Proc. 9th International Conference on Semiconductors, P. 1259, Moscow (1968).
35. H.K. Henisch et.al., J. Non-Cryst. Solids, 4(1970) 538.
36. H.K. Henisch et.al., Proc. International Congress on Thin Films, Paris (1970).
37. H.K. Henisch, Scientific America, 221 (1969) 30.
38. H. Fritzsche and S.R. Ovshinsky, J. Non-Cryst. Solids, 2 (1970) 393.

39. N.K. Hindley, J. Non-Cryst. Solids, 5 (1970) 31.
40. J.M. Ziman, Phil. Mag., 6 (1961) 1013.
41. A.F. Ioffe and A.R. Regel, Prog. Semiconductor, 4 (1960) 237.
42. P.W. Anderson, Phys. Rev., 109 (1958) 1492.
43. A.I. Gubanov (1963), 'Quantum Electron Theory of Amorphous Conductors', Consultants Bureau, New York, 1965.
44. L. Banyai (1964), Physique des Semiconducteurs (ed. M. Hulin), P. 417., Dunod, Paris.
45. N.F. Mott and E.A. Davis, 'Electronic Processes in Non-Crystalline Materials', Clarendon Press, Oxford, 1971.
46. M. Cohen, H. Fritzsche and S.R. Ovshinsky, Phys.Rev. Letters, 22 (1969) 1065.
47. E.A. Davis and N.F. Mott, Phil. Mag., 22 (1970) 903.
48. M. Kastner, Phys. Rev. Letters, 28 (1972) 355.
49. E.P. Denton, H. Rawson and J.E. Stanworth, Nature, London, 173 (1954), 10.
50. J.D. Mackenzie, 'Semiconducting Oxide Glasses' in 'Modern Aspects of the Vitreous State', Ed. J.D. Mackenzie, Vol. 3 (1964), Butterworths (Washington).
51. J.D. Mackenzie, J.Am. Ceram. Soc., 47 (1964) 211.
52. D.P. Han-blen et.al. J. Am. Ceram. Soc., 46 (1963) 499.
53. M. Munakata, Solid State Electronics, 1 (1960) 159.
54. M. Munakata and M. Iwamoto, J. Ceram. Assocn. Japan, 68 (1960) 125.
55. P.L. Baynton et.al., J. Electrochem. Soc., 104 (1957) 237.
56. V. A. Ioffe et.al., Sov. Phys. - Solid State, 2(1960)609.
57. B.V. Janakirama Rao, J.Am. Ceram. Soc., 48 (1965) 311.
58. K.W. Hansen, J. Electrochem. Soc., 112 (1965) 994.

59. T.N. Kennedy and J.D. Mackenzie, Phys. Chem. Glasses, 8 (1967).
60. R. Tsu et.al., J. Non-Cryst. Solids, 4 (1970) 322.
61. A.M. Andriesh and B.T. Kolomiets, Soviet Phys. Solid State, 6 (1965) 2652.
62. M.H. Bodsky et.al., Phys. Rev. B1, (1970) 2632.
63. H.L. Uphoff and J.H. Healy, J.Appl.Phys., 32 (1961) 950.
64. B.T. Kolomiets, Phys. Stat. Solidi, 359 (1964) 713.
65. N.S. Platakis et.al., J. Electrochem. Soc., 116 (1969) 1436.
66. J.T. Edmond, J. Appl. Phys., 17 (1966) 979.
67. J.T. Edmond, J. Non-Cryst. Solids, 1 (1968) 39.
68. A.E. Owen and J.M. Robertson, J. Non-Cryst. Solids, 4 (1970) 117.
69. J.I. Polanco and G.G. Roberts, Phil. Mag., 27 (1972) 217.
70. A.H. Clark, Phys. Rev., 135 (1967) 75.
71. J.I. Polanco and G.G. Roberts, Phil. Mag., 25 (1972) 117.
72. M. Pollak, Phil. Mag. 23 (1971) 519.
73. J. Schnakenberg, Phys. Status Solidi, 28 (1968) 623.
74. G.N. Greaves, J. Non-Cryst. Solids, 11 (1973) 427.
75. A.F. Schmid, Jour. Appl. Phys., 40 (1969) 4128.
76. J.O. Isard, J. Non-Cryst. Solids, 4 (1970) 357.

29505

ME-1974-M-BAN-ELE